Formation and evolution of Bright Central Galaxies in the core of massive galaxy clusters

Paolo Tozzi - INAF OAA

Dynamical complexity in astrophysical contexts - IFPU, Trieste 6-10 February 2023

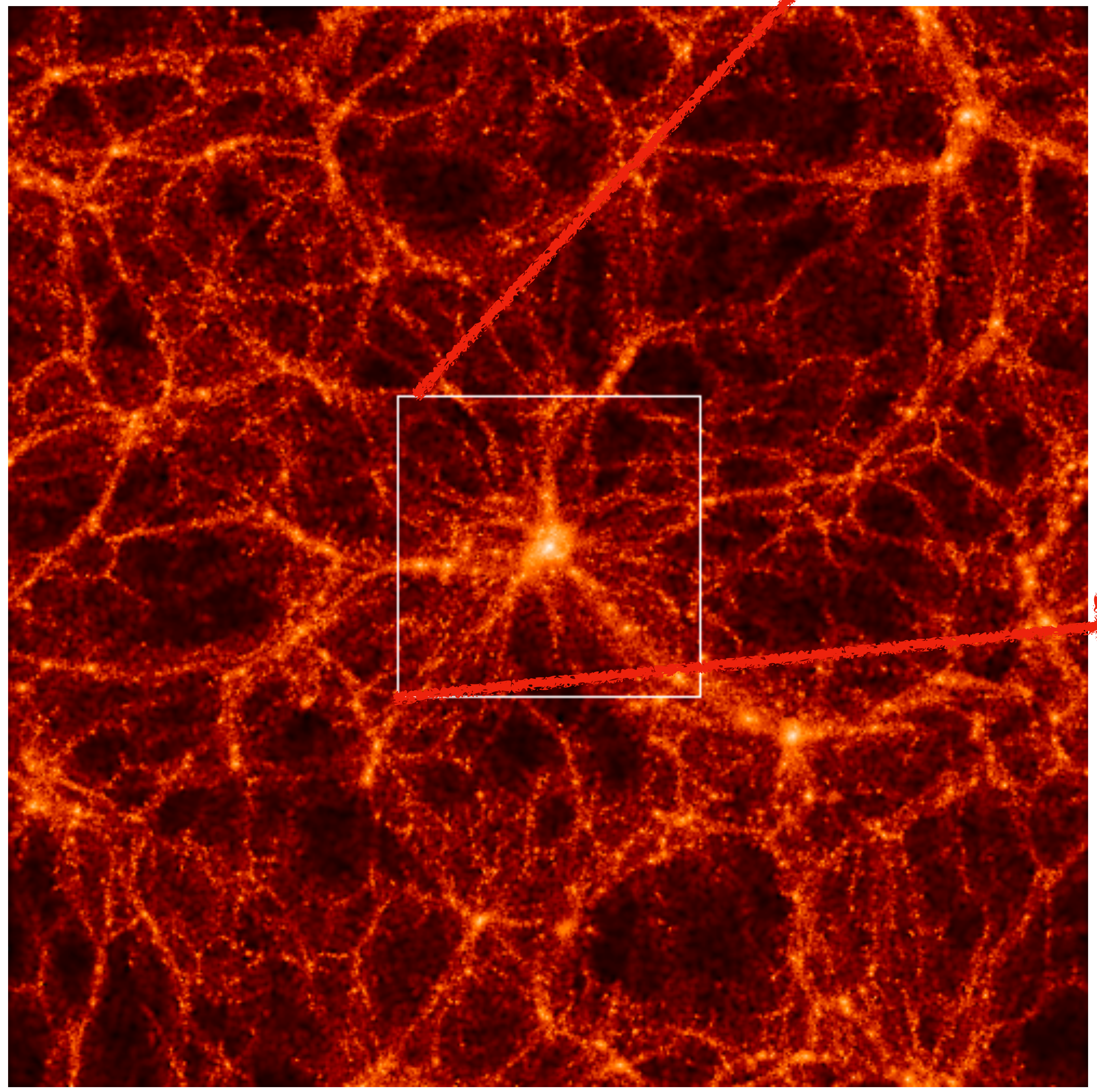

Springel et al. 2000 - GADGET

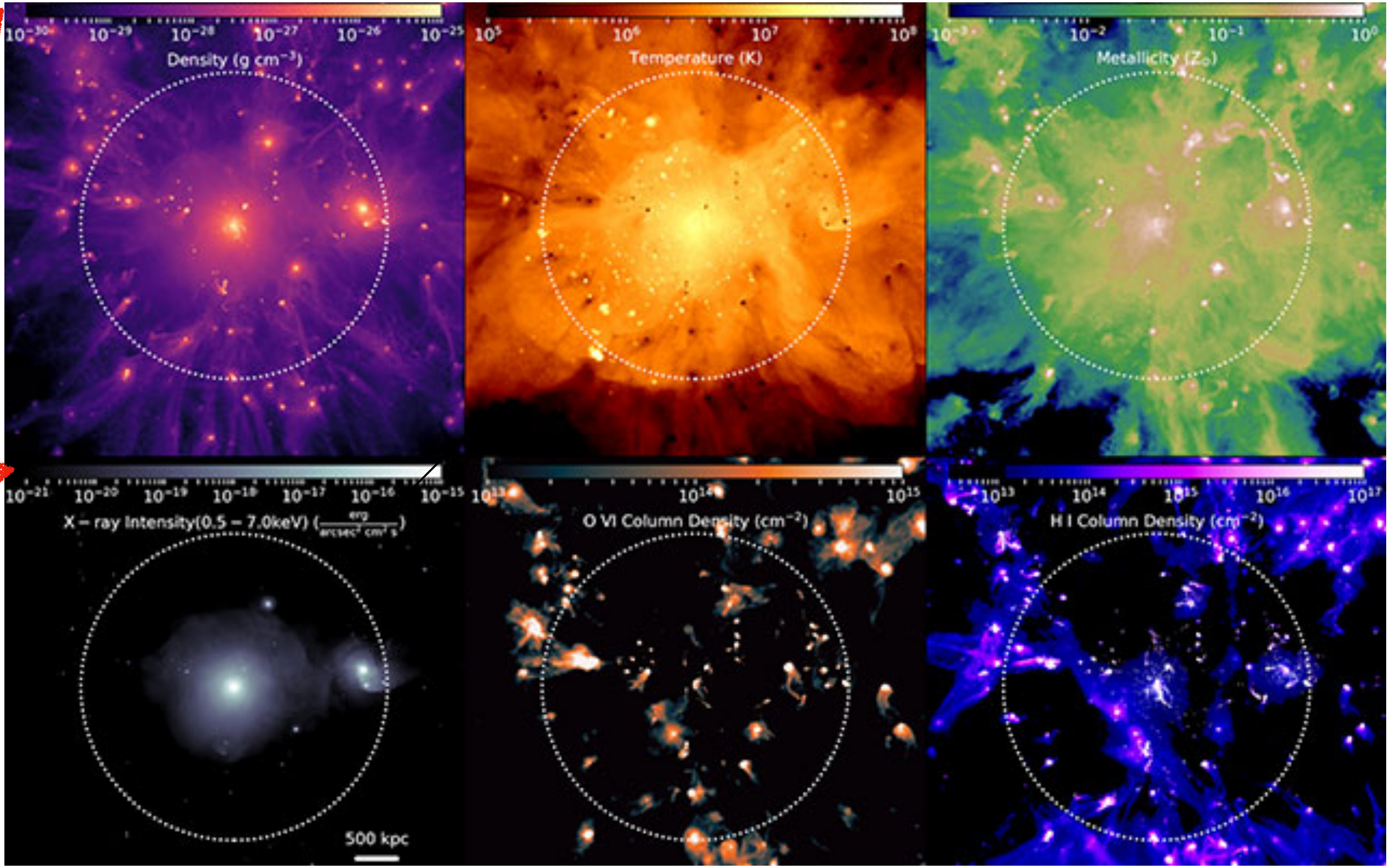

Butsky et al. 2020

Galaxy cluster mass partitioning

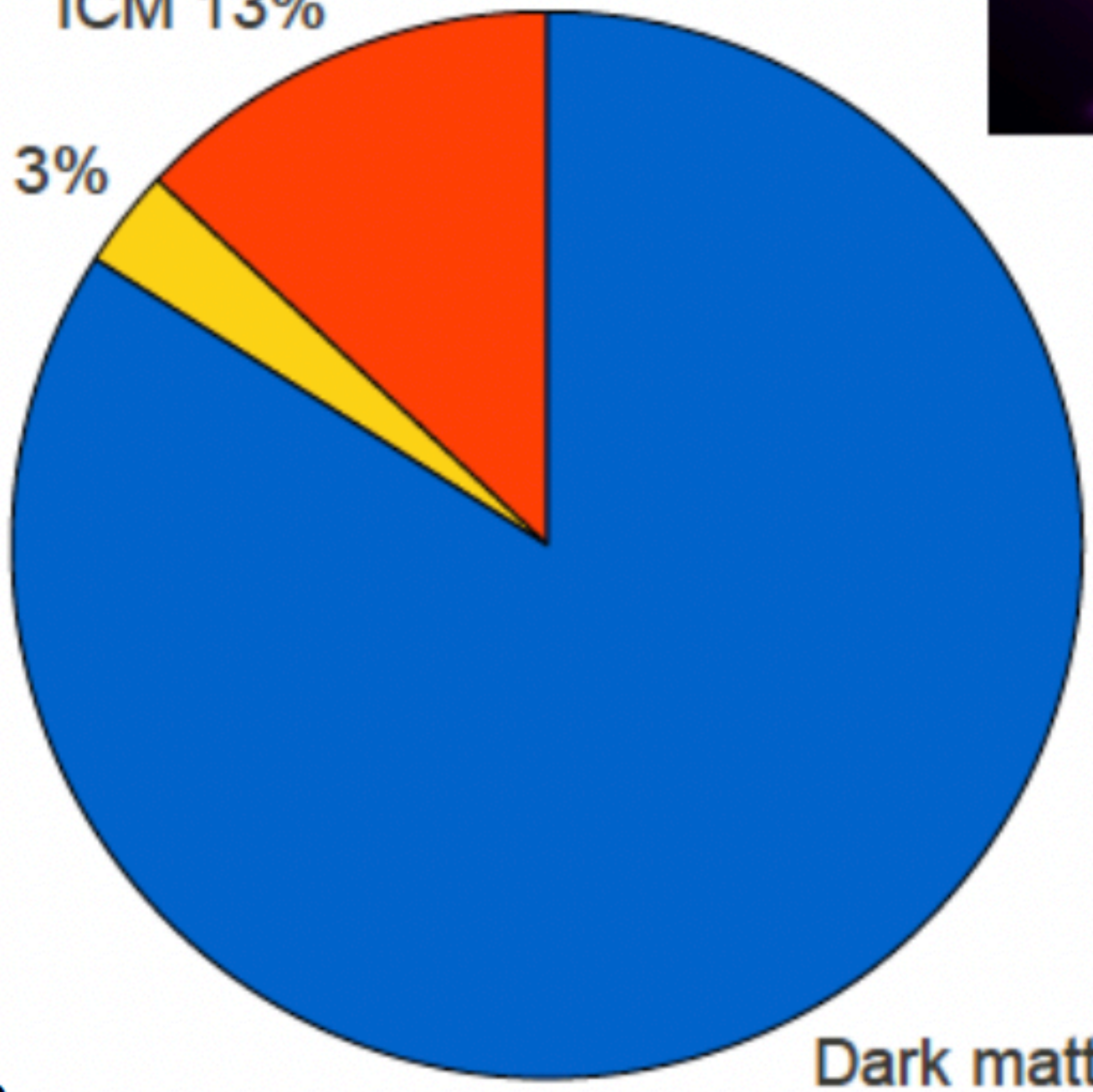

Credit: Abell 1689, X-ray: NASA/CXC/MIT/
E.-H Peng et al.; Optical: NASA/STScl

B. McNamara

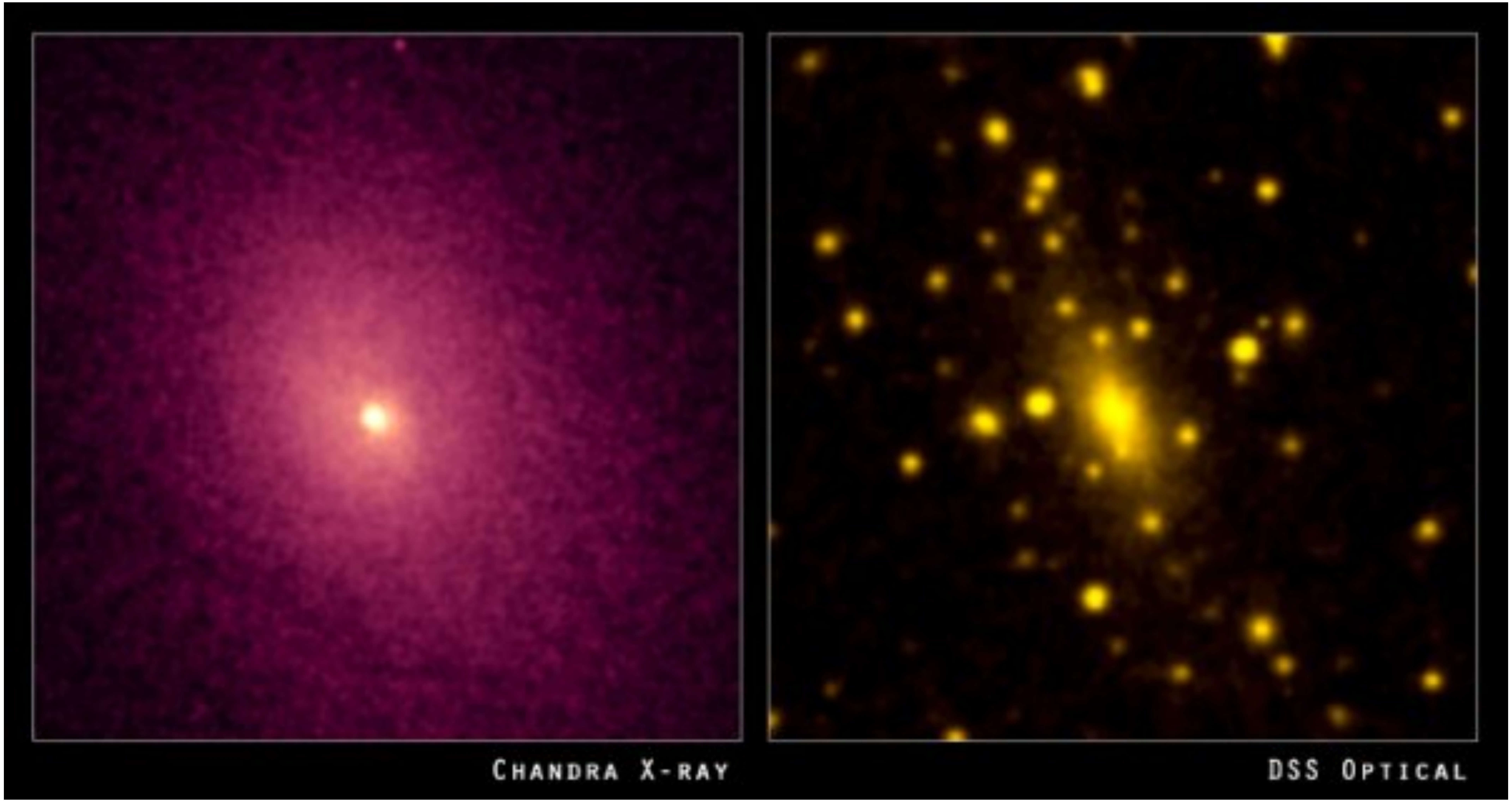
CHANDRA X-RAY
DSS OPTICAL

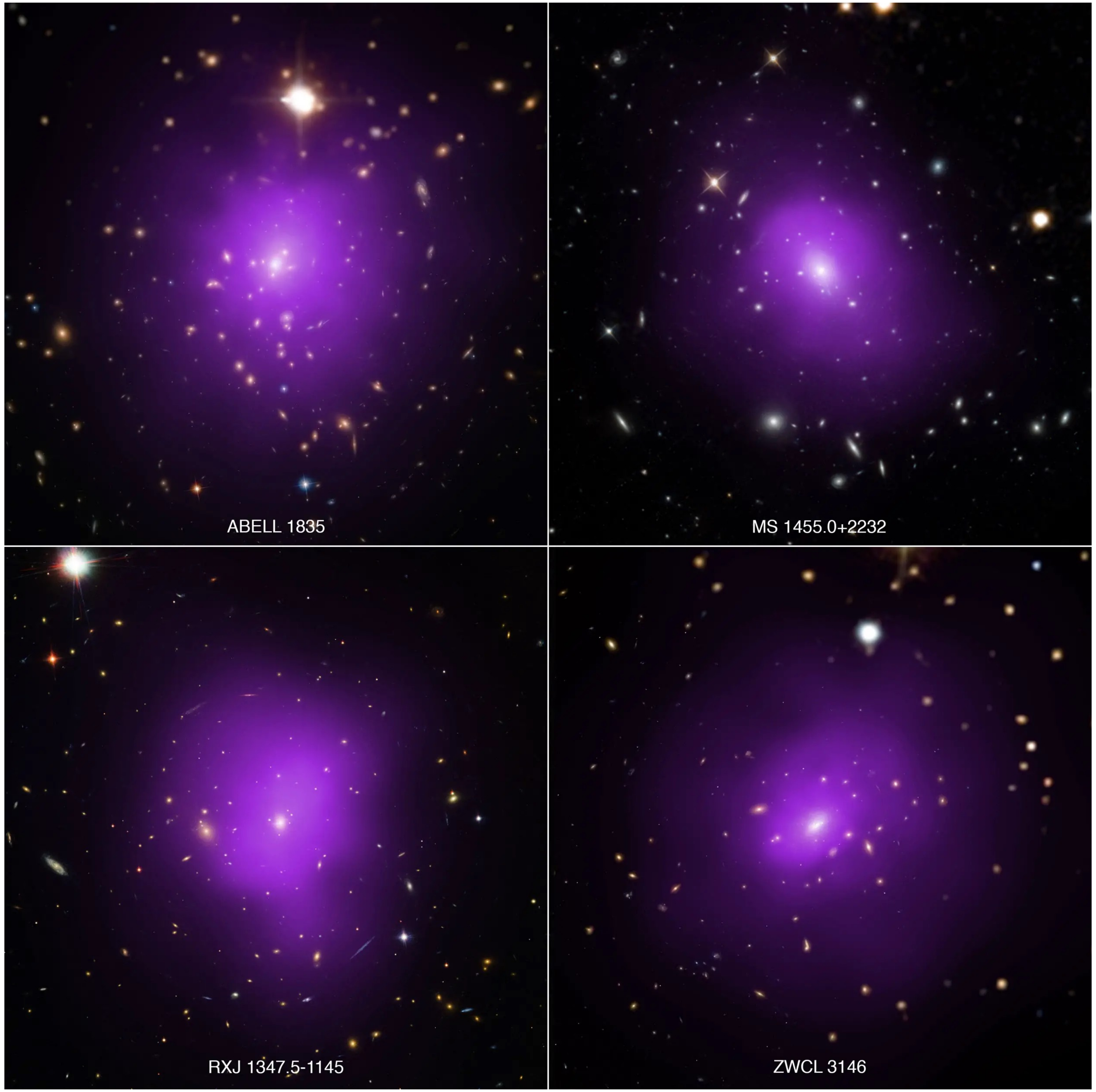
ABELL 1835
MS 1455.0+2232
RXJ 1347.5-1145
ZWCL 3146

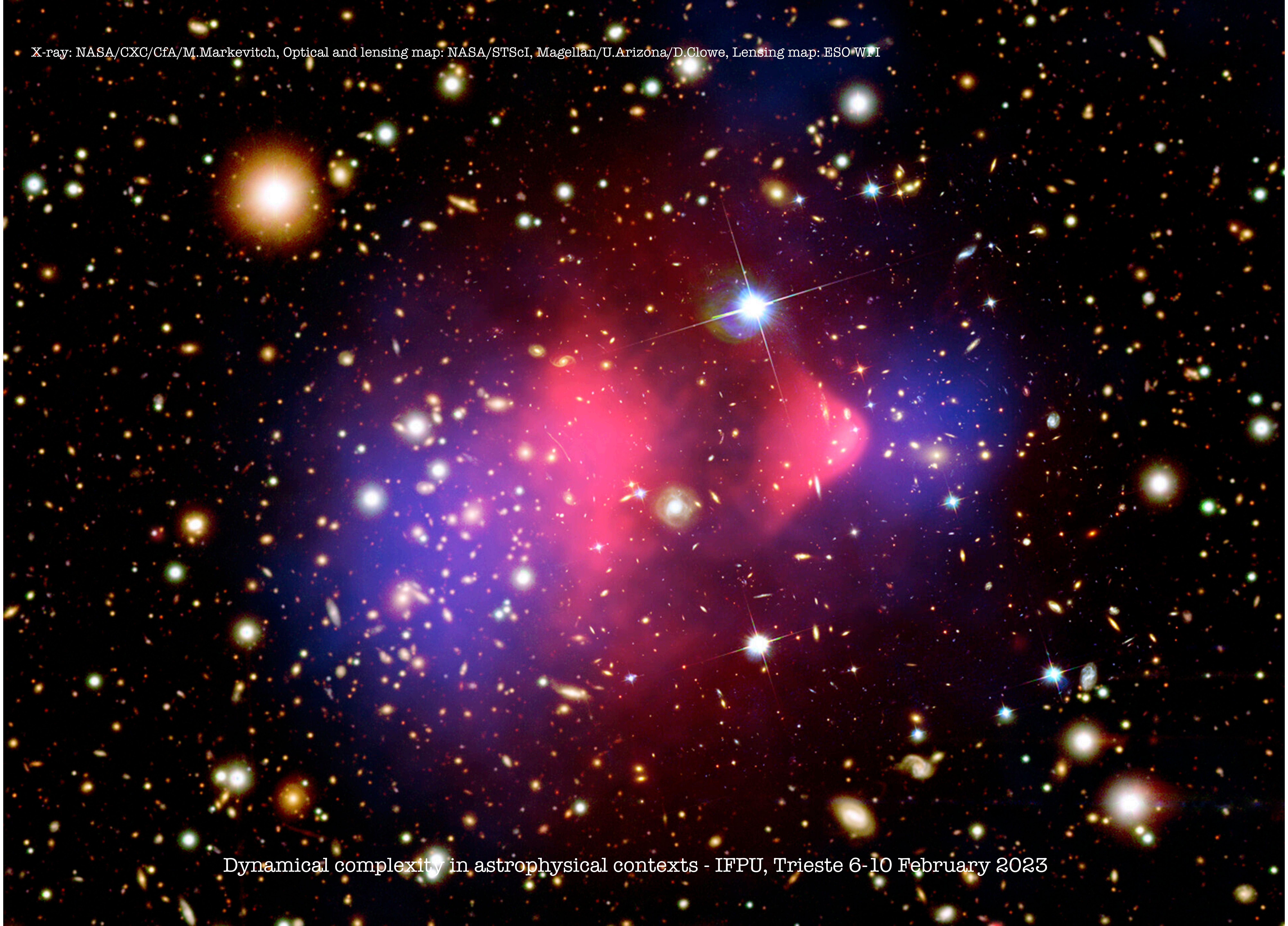
X-ray: NASA/CXC/CfA/M.Markevitch, Optical and lensing map: NASA/STScI, Magellan/U.Arizona/D.Clowe, Lensing map: ESO WFI
Dynamical complexity in astrophysical contexts - IFPU, Trieste 6-10 February 2023

$$t_{\rm cool} \simeq \frac{3}{2}\frac{nkT}{n_{\rm e}n_{\rm i}\Lambda(Z,T)}$$

$$\frac{dL_x}{dT_K} = \frac{5}{2}\frac{\dot{M}k}{\mu m_p}.$$

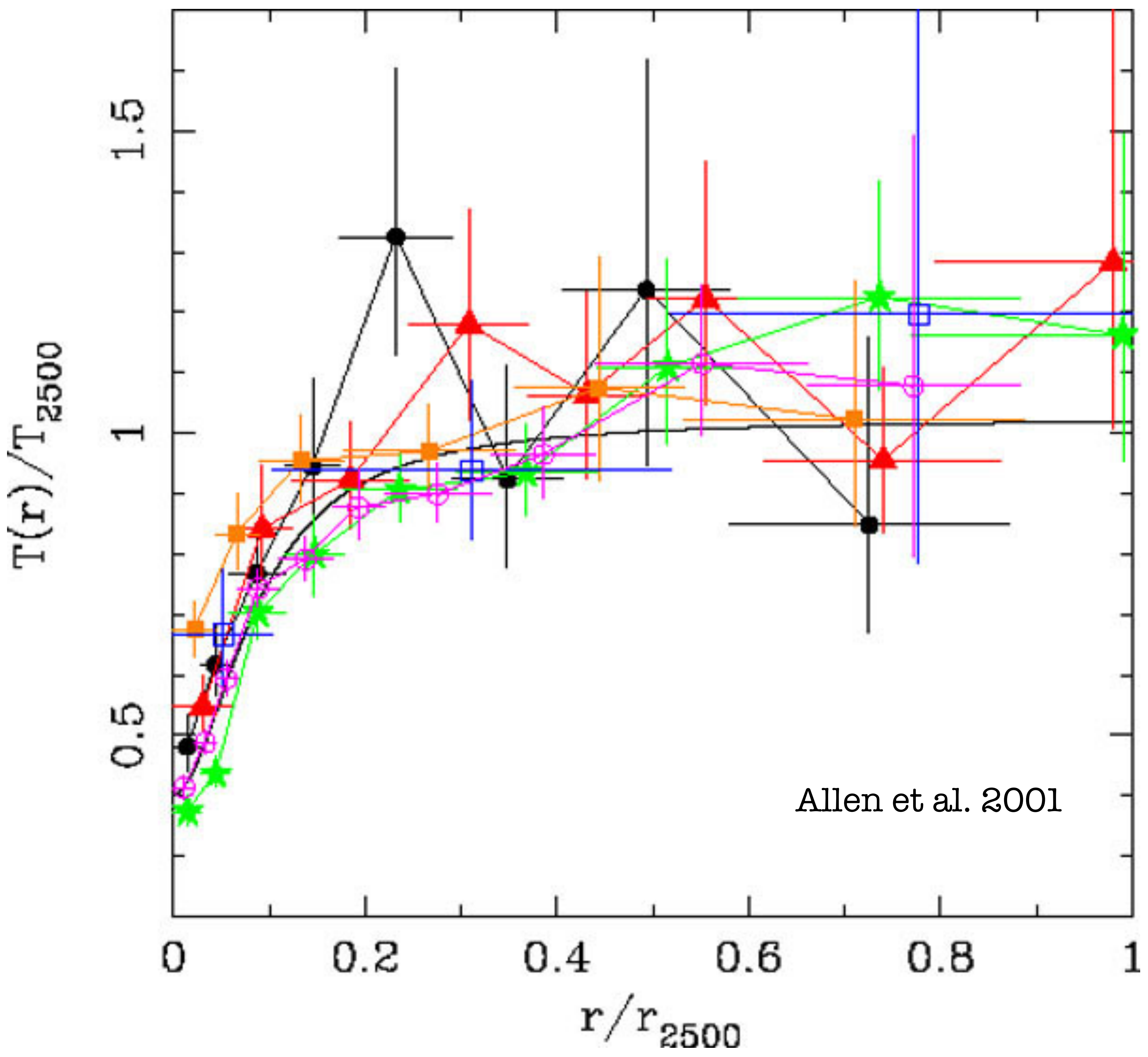

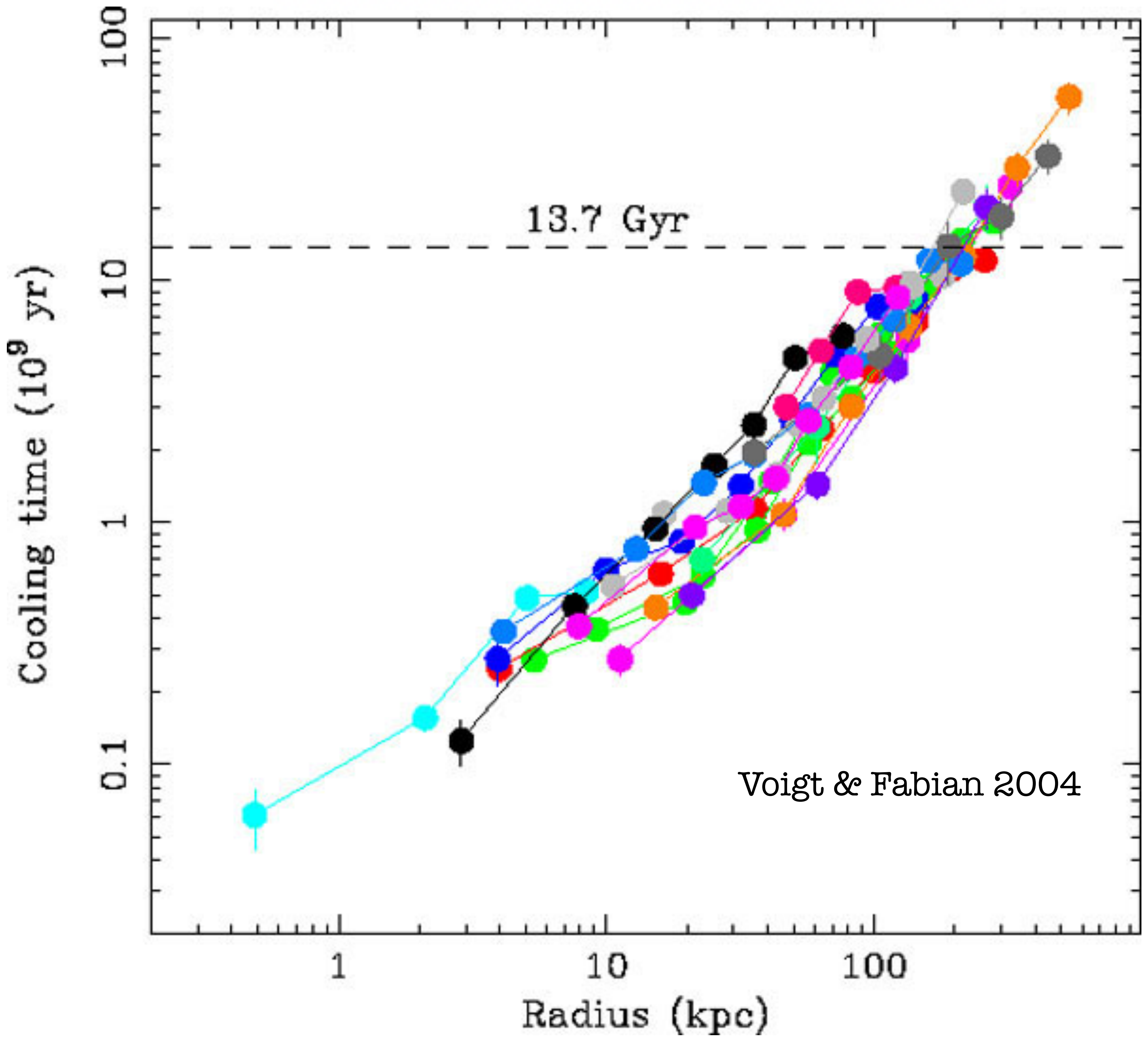

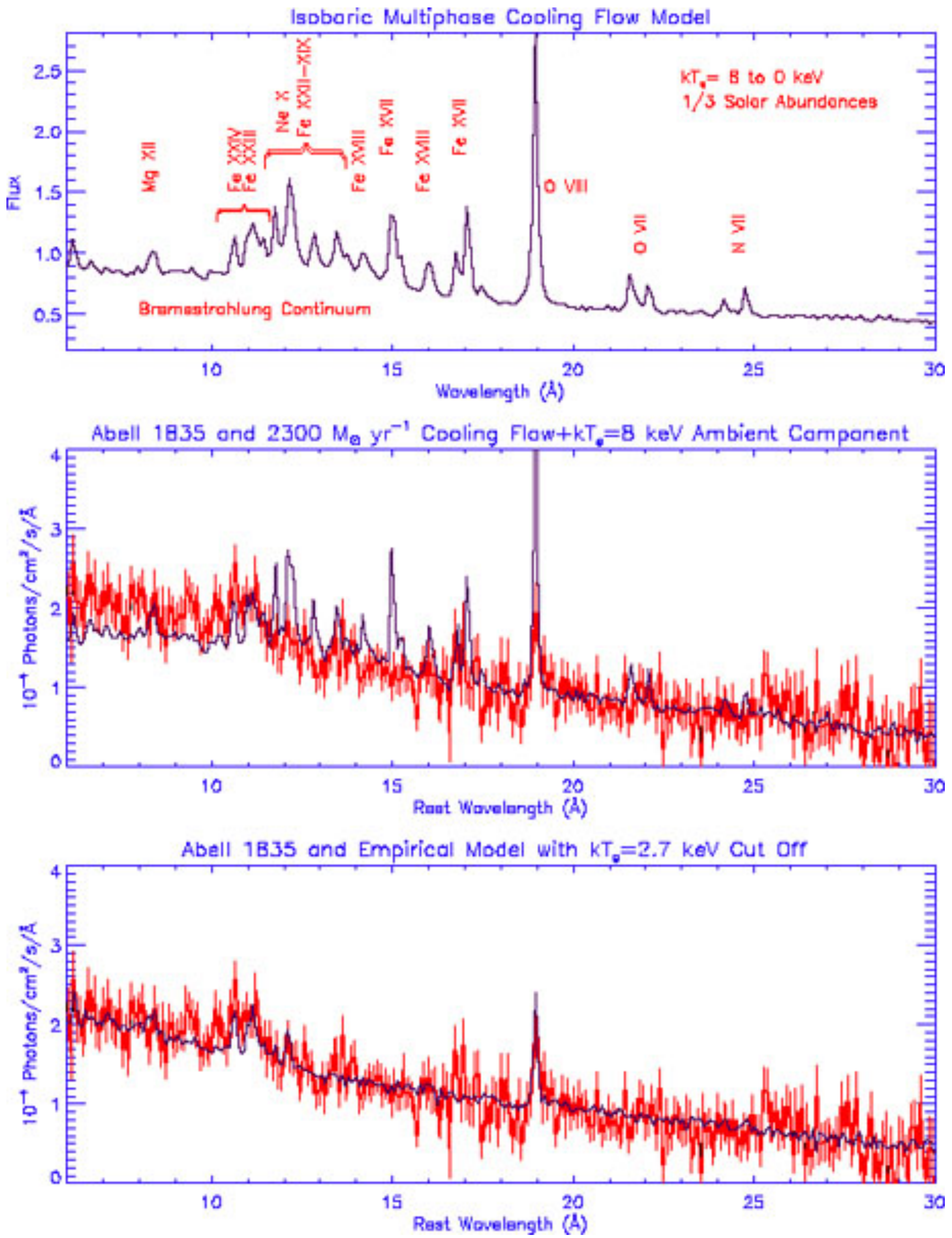

$$\frac{dL_x}{dT_K} = \frac{5}{2}\frac{\dot{M}k}{\mu m_p}.$$

Peterson et al. 2001

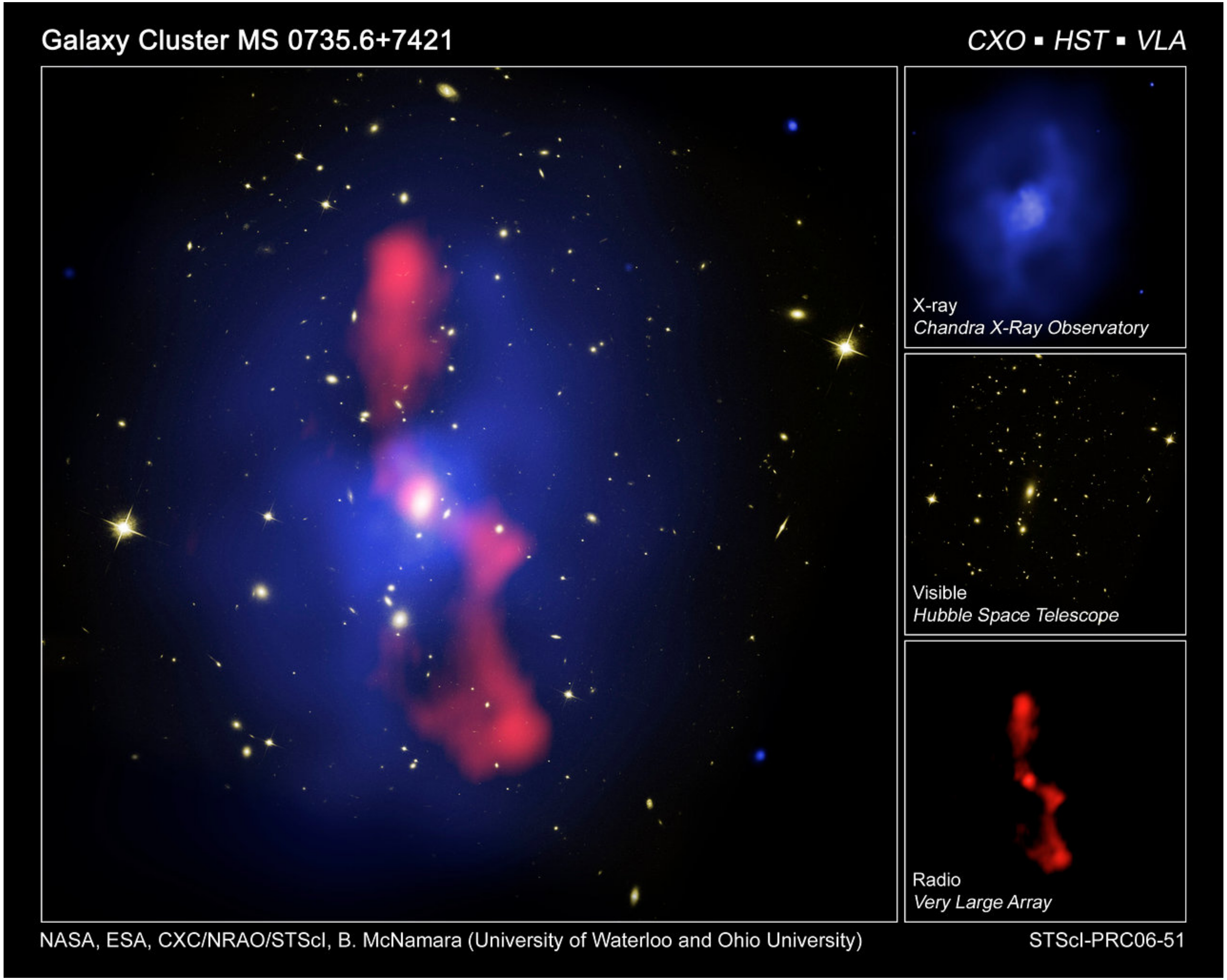
Galaxy Cluster MS 0735.6+7421
CXO ▪ HST ▪ VLA
X-ray
Chandra X-Ray Observatory
Visible
Hubble Space Telescope
Radio
Very Large Array
NASA, ESA, CXC/NRAO/STScI, B. McNamara (University of Waterloo and Ohio University)
STScI-PRC06-51

SFR larger than isobaric mass deposition rate allowed by the X-ray spectrum in MACSJ1931

$$\frac{dL}{dT} \propto \frac{5}{2} \frac{\dot{M}\,k}{\mu\, m_p}$$

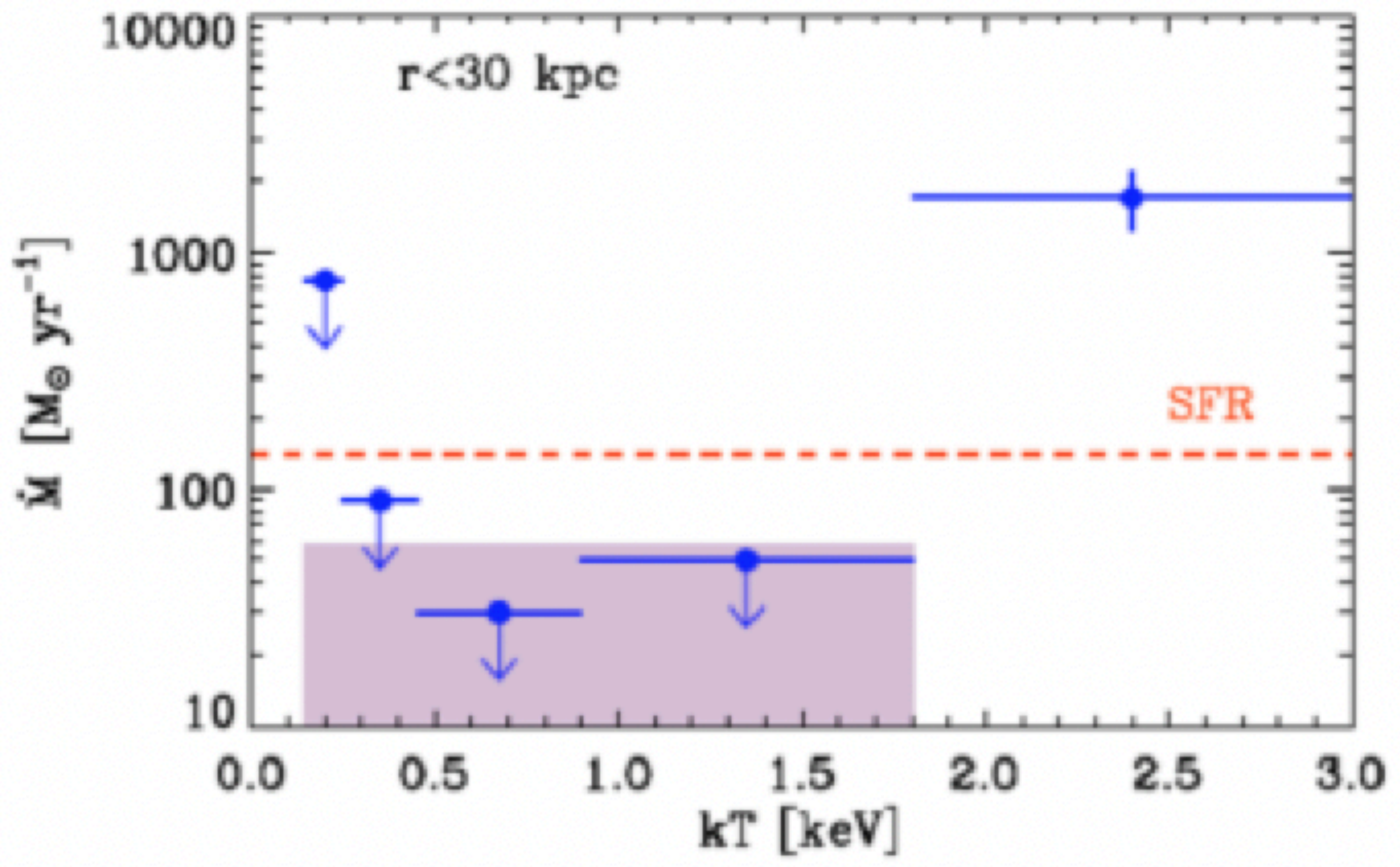

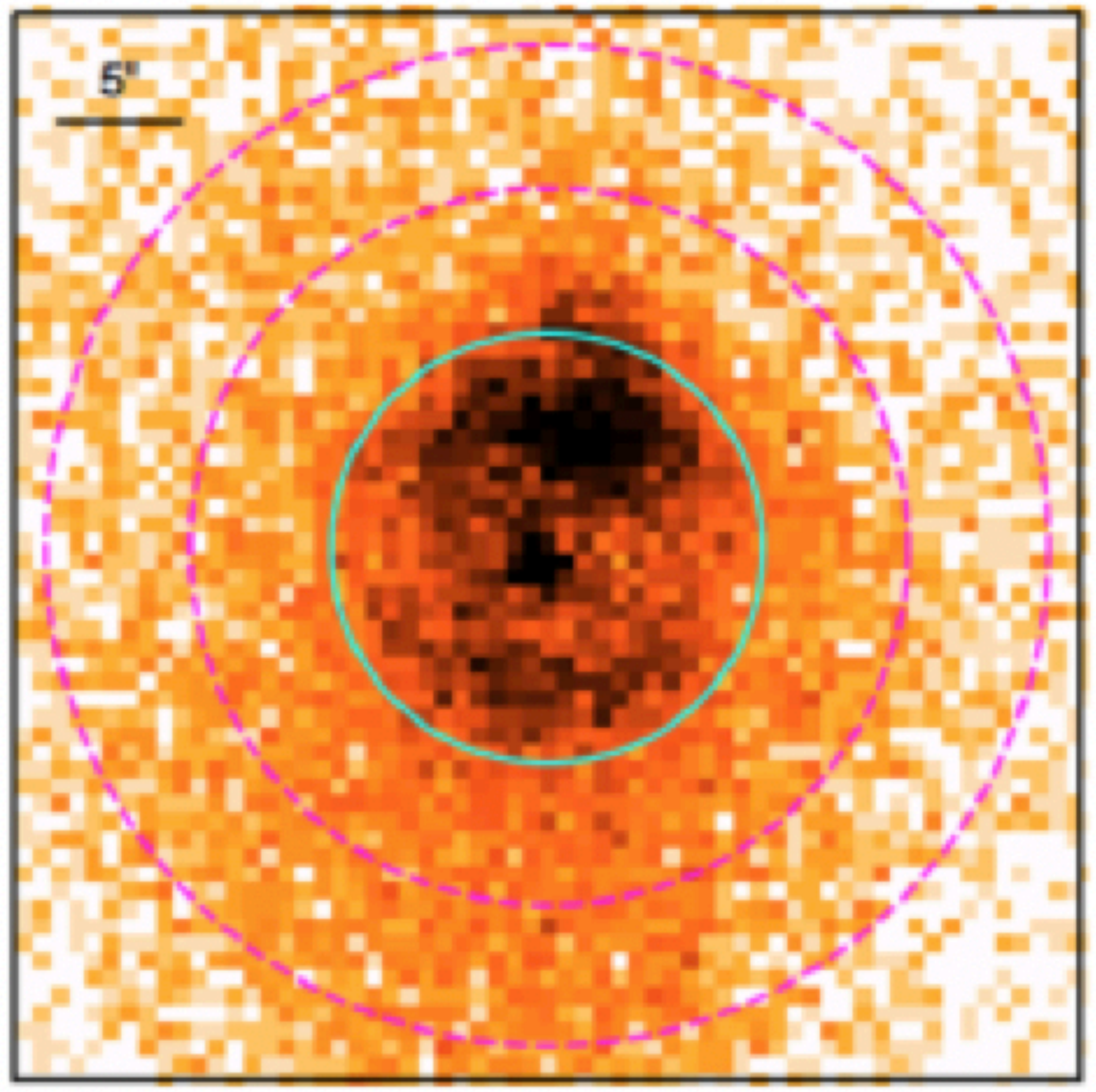

Santos et al. (2016)

Limits on the isobaric cooling rate in cool core clusters

Name	z	*SFR* $M_\odot$ yr^{-1}	SFR Orig.[a]	SFR Ref.[b]	M_{mol}[c] $10^{10}\ M_\odot$	M_{mol} Ref.[d]
A1835	0.252	146	IR SED	Ra12	5.0	Mn14
RXC J1504.1	0.215	140	H_α	Og10	–	–
RX J1532.9+3021	0.345	110	70 μm	Ho12	12.5[e]	Ed01
A1068	0.139	99.3	IR SED	Ra12	3.7[f]	Sa03
ZW 3146	0.291	93.1	IR SED	Ra12	8.0[e]	Ed01
Z0348	0.254	32.6	IR SED	Ra12	–	–

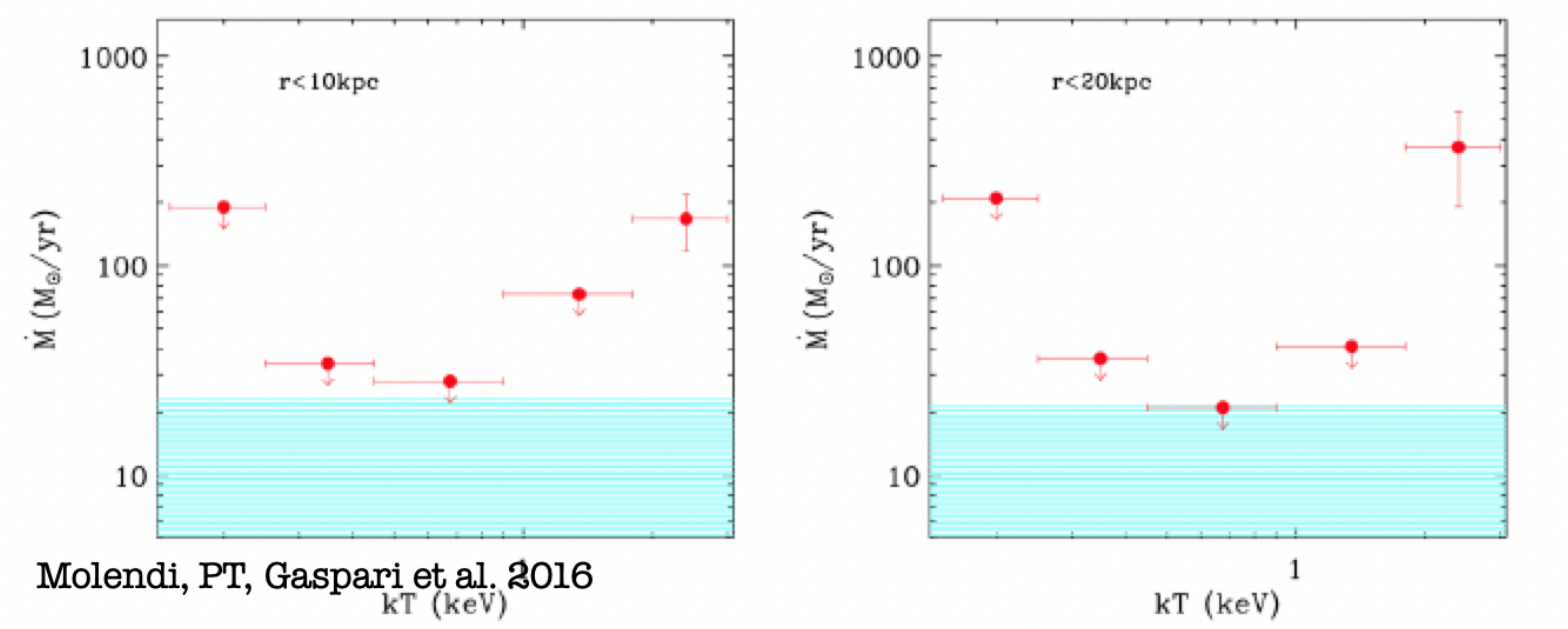

Molendi, PT, Gaspari et al. 2016

Current limits on isobaric cooling flows are lower than observed SFR. Way out: SF events naturally slower and non-isobaric cooling

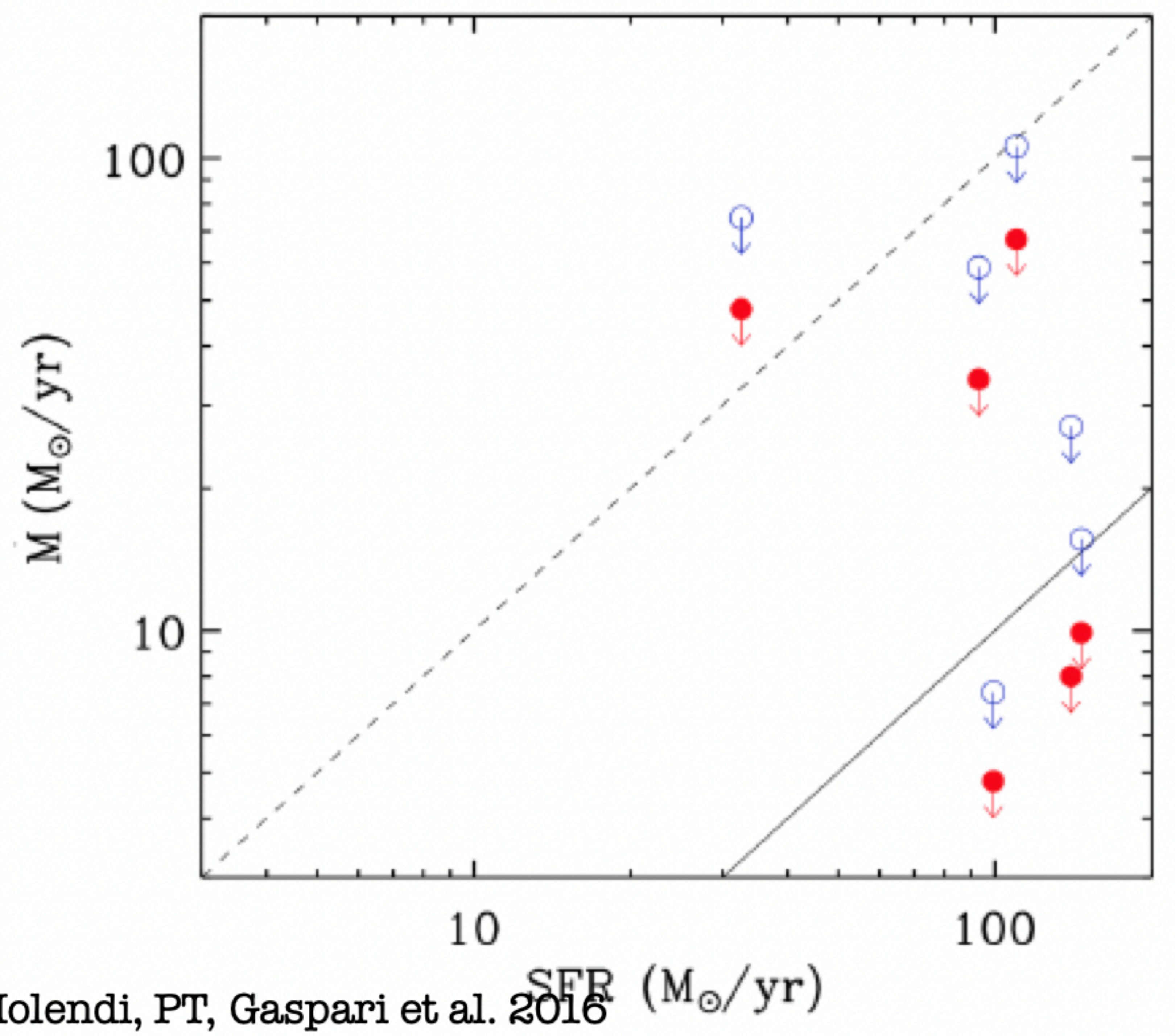

Molendi, PT, Gaspari et al. 2016

CLJ1415, z=1.0, the strongest cool core at z~1

CL1415 field
ACIS-I+ACIS-S 80+270 ks (Santos et al. 2012)

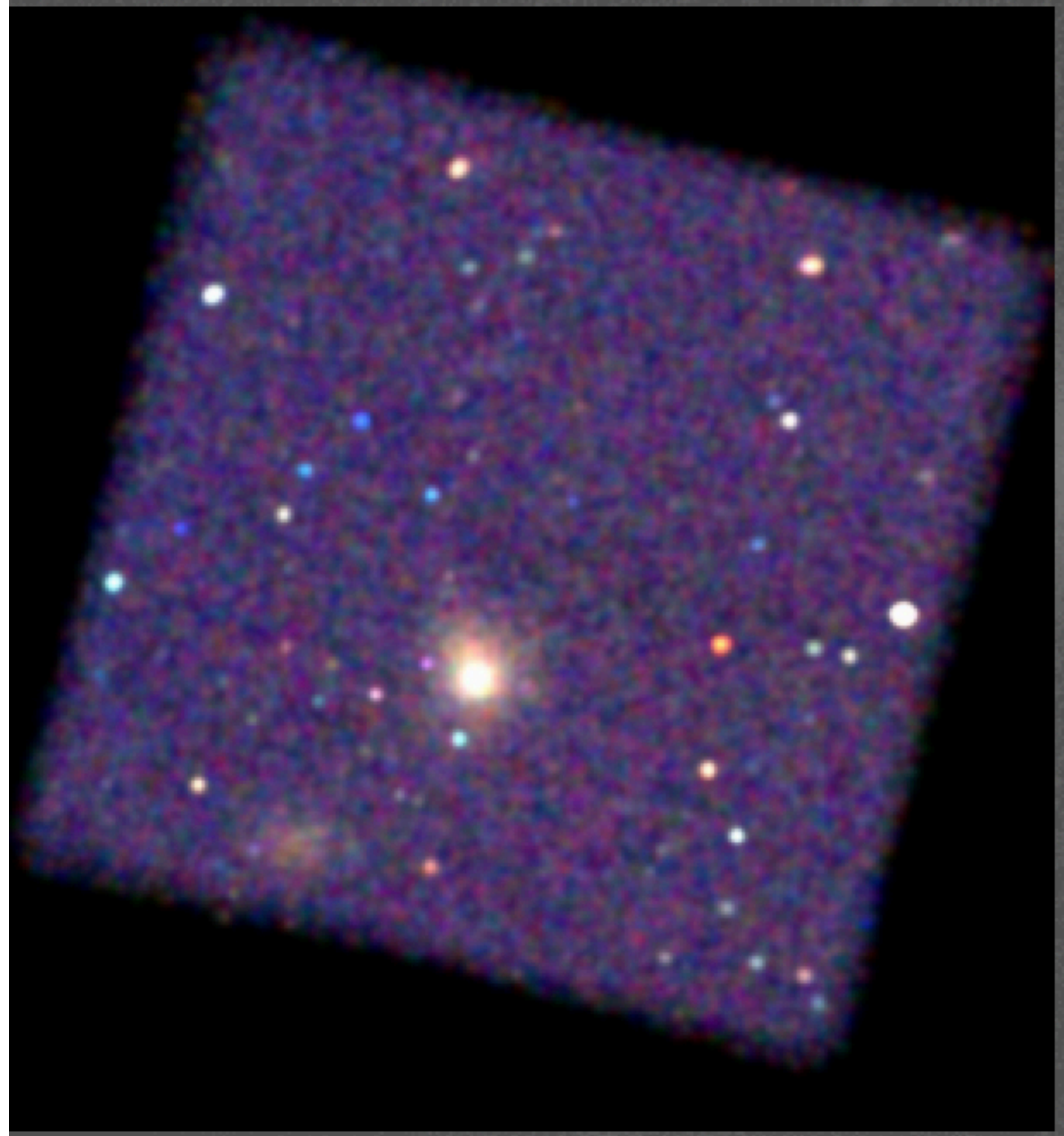

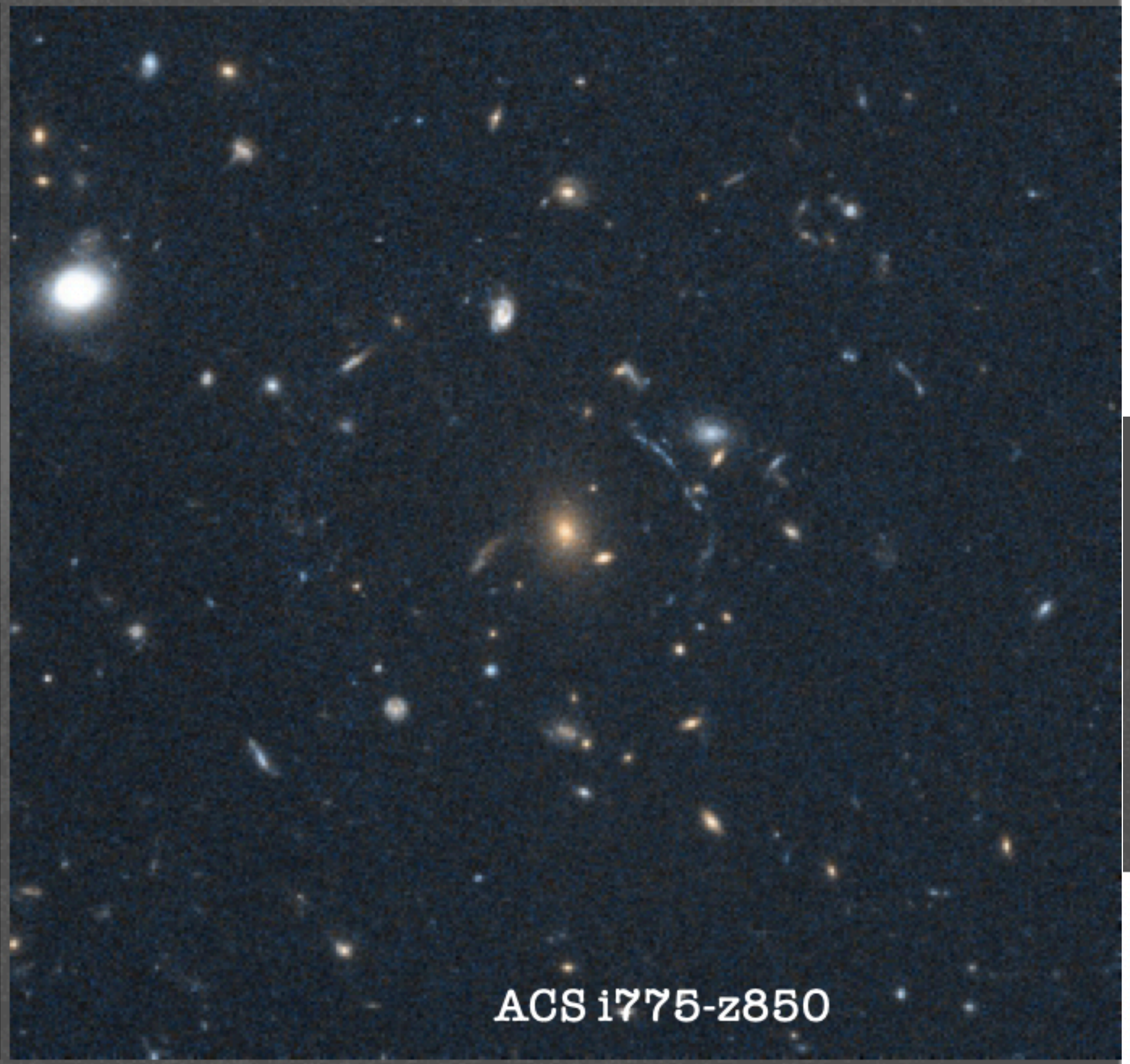

CL1415 @ z=1, a CC in the distant Universe

Angular resolution ~ 25 kpc in the inner regions
About 7000 net photons with Chandra

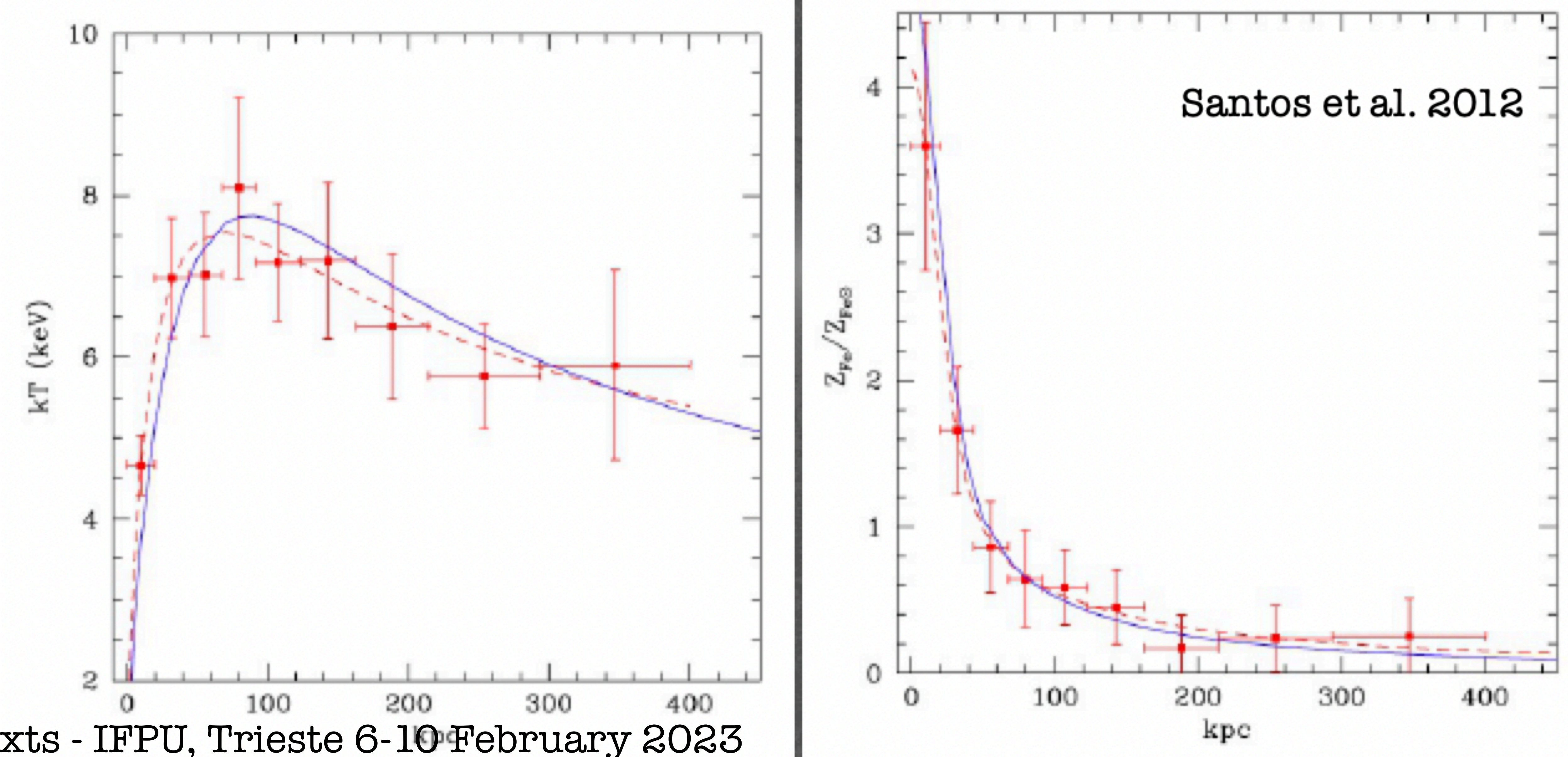

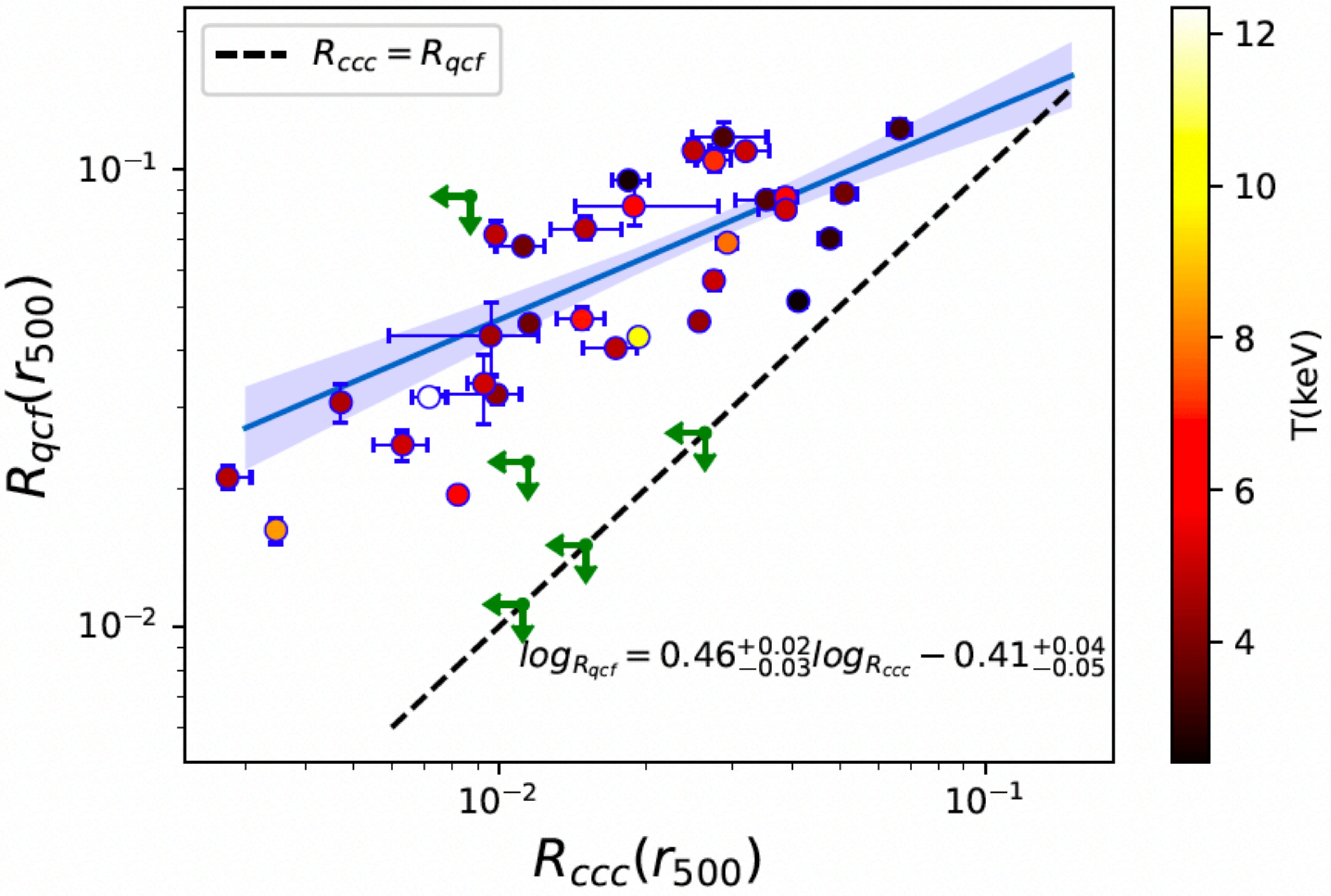

Wang et al. 2023

Cool cores and mass flows open issues:

Isobaric cooling flows are not observed in the large majority of the cases - can they still happen on a short time scale?

Note: Some more sophisticated models of cooling flow, called hidden cooling flow, can still allow significant mass deposition rate, but this bring back again the missing mass problem (solution with fragmentation into very small objects?)

Residual stellar formation episodes are observed in BCG, but it is not clear if this is from cold gas from within cluster galaxies, or if it is cooling from the hot phase.

Is there a clear connection/continuity across the cooling ladder:
1 keV —> Halpha (10^4) —> CO (molecular)?

The coupling mechanism between the radio-mode feedback and the surrounding ICM is not fully understood

The triggering mechanism of the nuclear feedback is not understood.

Overall, we do not have a comprehensive framework for the baryon cycle, the time scale and the energy budget of the feedback

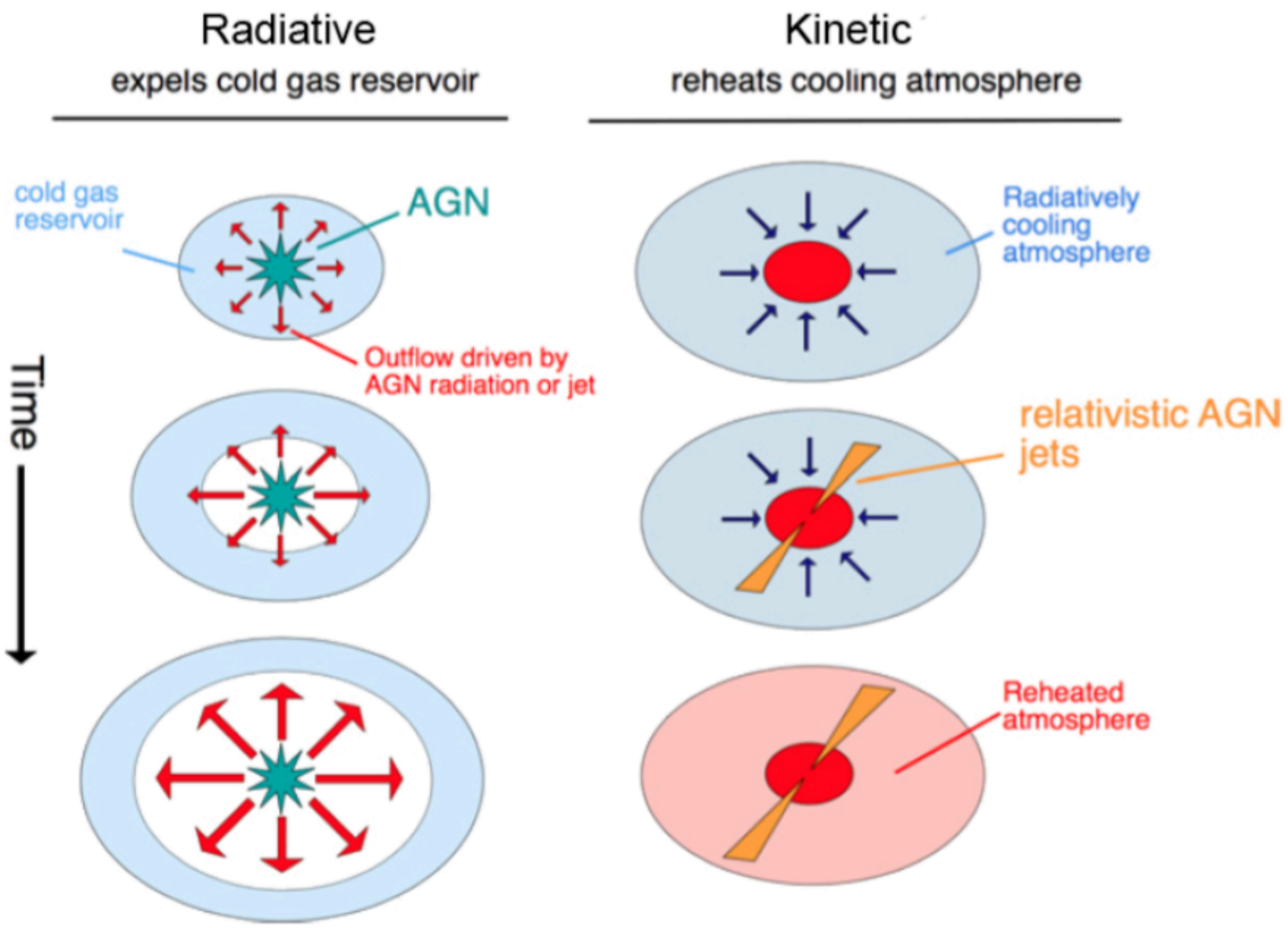
Radiative
expels cold gas reservoir
Kinetic
reheats cooling atmosphere
cold gas reservoir
AGN
Outflow driven by AGN radiation or jet
Time
Radiatively cooling atmosphere
relativistic AGN jets
Reheated atmosphere

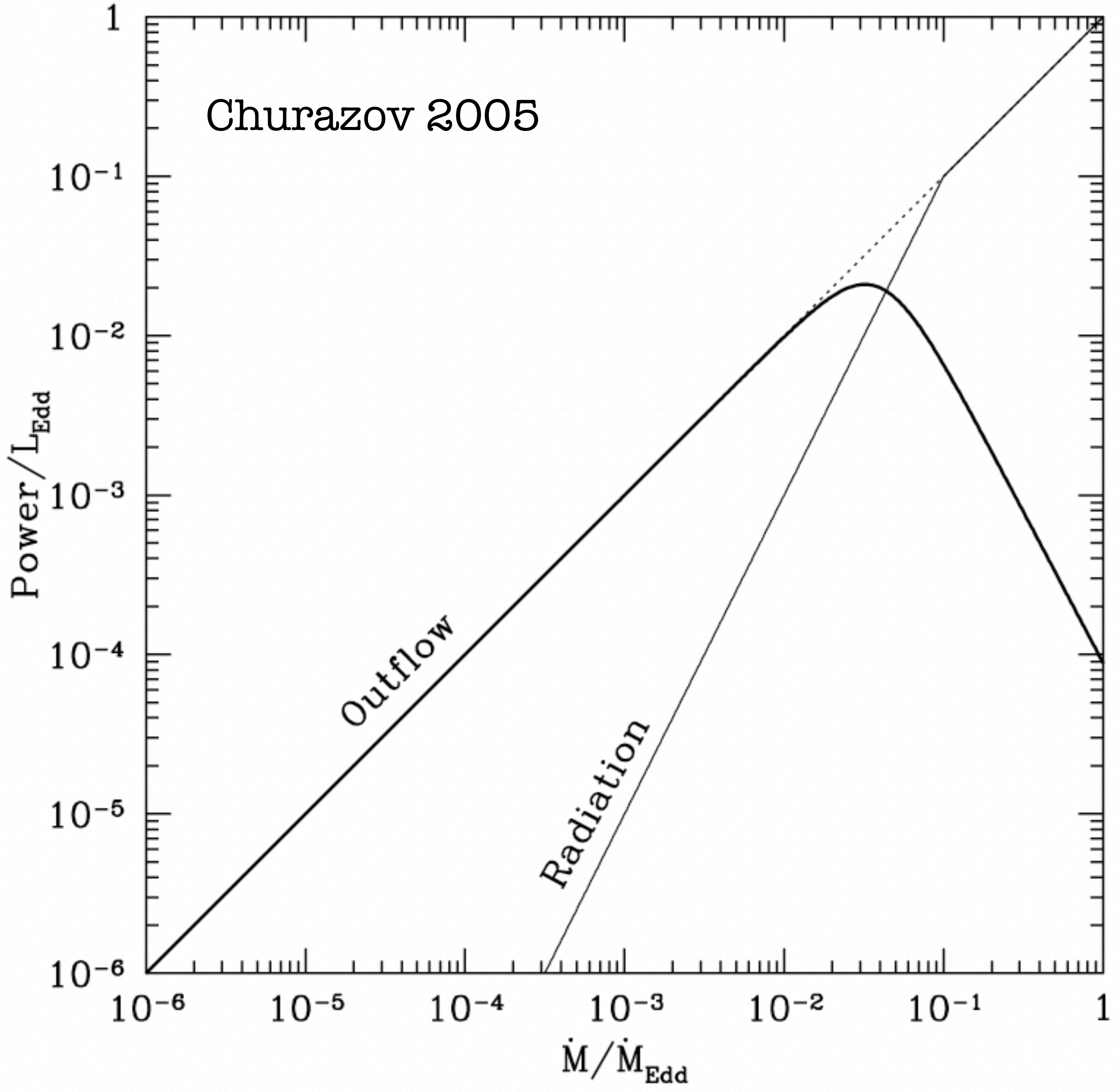

The transition between the radiatively efficient accretion regime and the radiatively inefficient flow typically occurs around one per cent of the Eddington rate ($\lambda \sim 0.01$), below which the kinetic output dominates over the radiative output (e.g. Churazov et al. 2005). Most of the objects in our radio-AGN sample have low

As already mentioned, the relative importance of radiative versus kinetic feedback modes seems to be regulated by the accretion state. At high accretion rates, close to the Eddington limit, the radiative efficiency is high and the radiative output dominates over the kinetic output (Churazov et al. 2005). However, at low accretion rates, the radiative efficiency drops dramatically, and the bulk of the energy is released in kinetic form via radio jets. The latter mode of feedback, characterized by low radiative efficiency, is thought to be the primary mode operating in the most massive galaxies in the present-day Universe. Indeed our sample of local radio-AGN is

Ishibashi et al. 2014

The Astrophysical Journal, 859:65 (24pp), 2018 May 20 https://doi.org/10.3847/1538-4357/aabfd7

X-Ray Properties of AGN in Brightest Cluster Galaxies. I. A Systematic Study of the *Chandra* Archive in the $0.2 < z < 0.3$ and $0.55 < z < 0.75$ Redshift Range

Lilan Yang[1], Paolo Tozzi[2,1], Heng Yu[1], Elisabeta Lusso[3], Massimo Gaspari[4,7], Roberto Gilli[5], Emanuele Nardini[2], and Guido Risaliti[2,6]

Yang et al. 2018

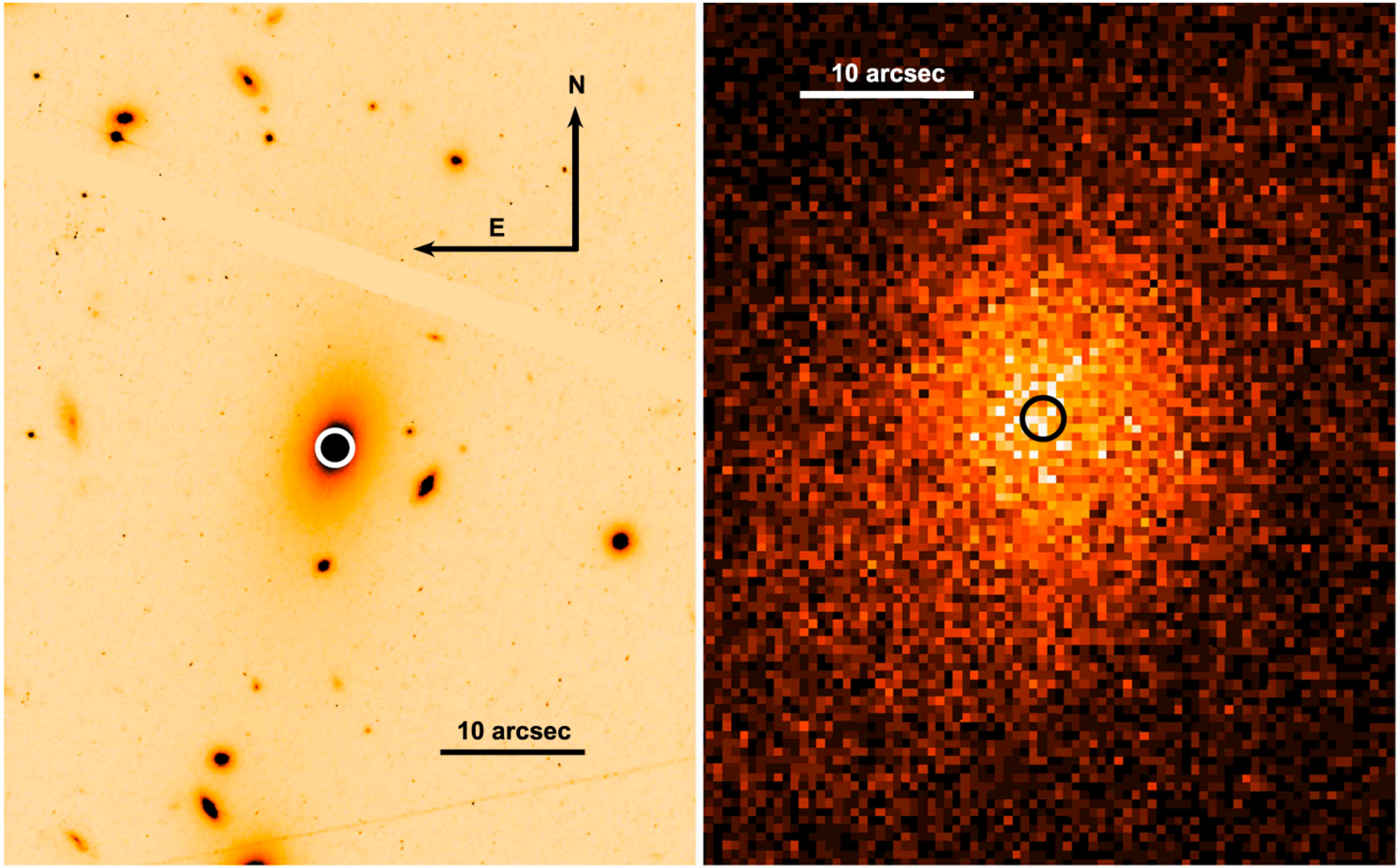

Yang et al. 2018

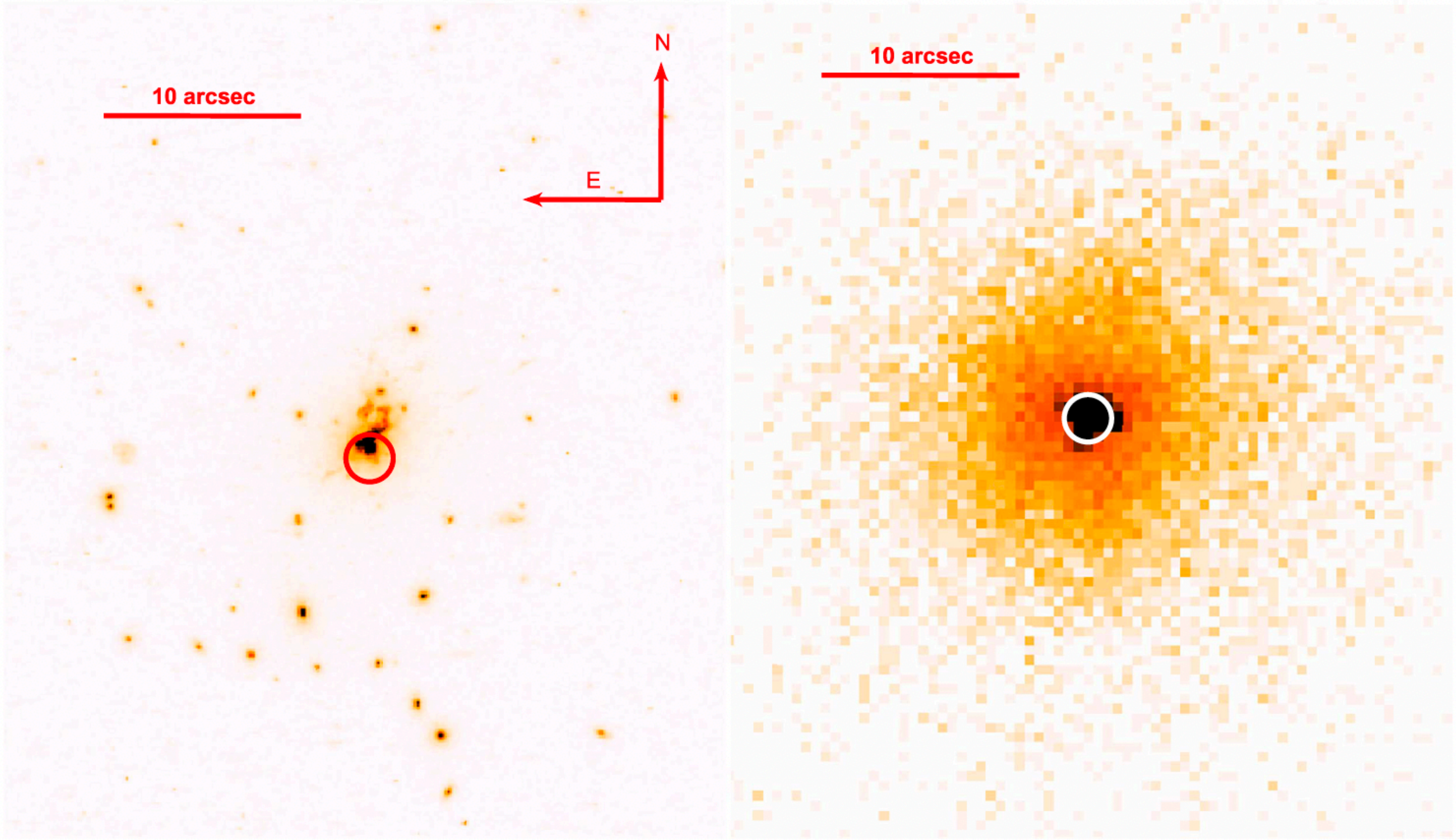

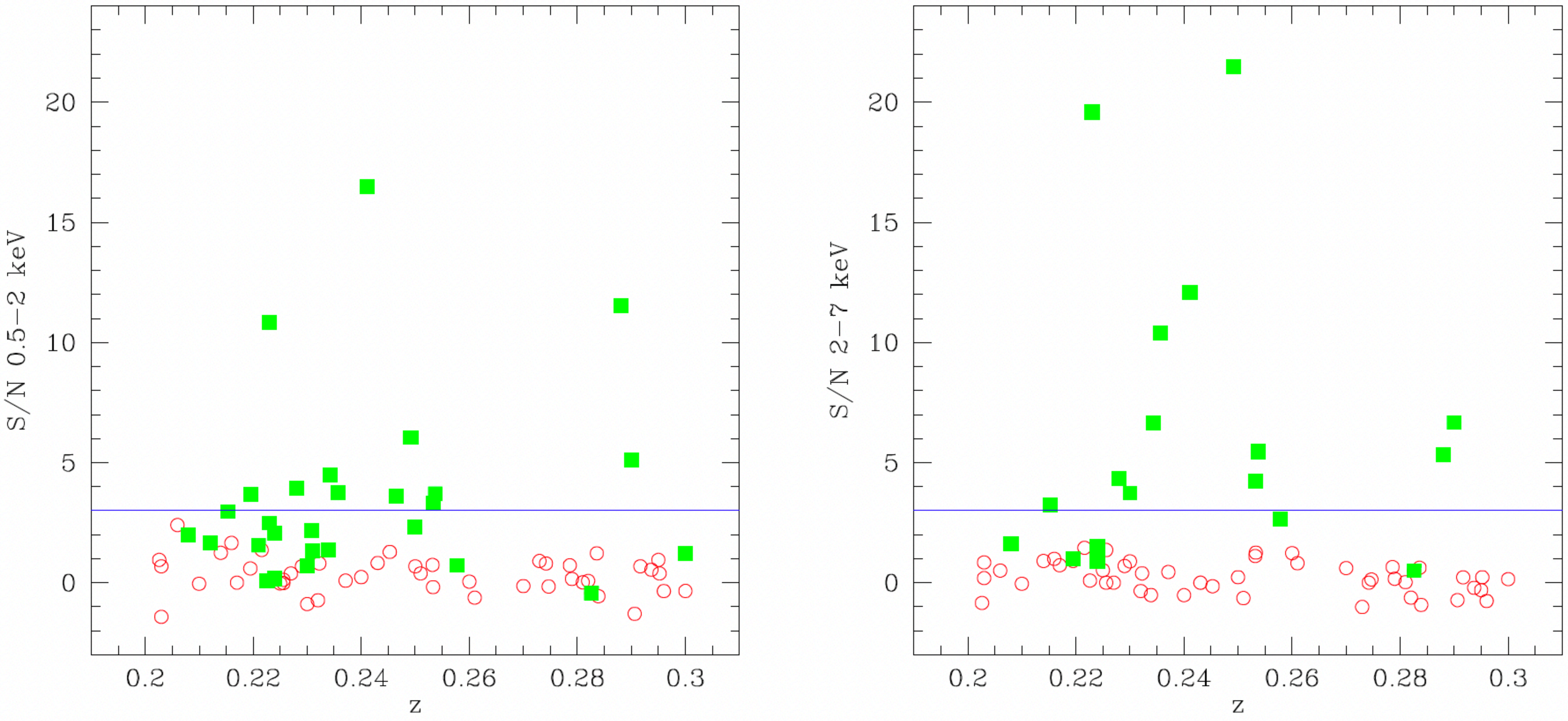

S/N 0.5−2 keV
z
S/N 2−7 keV
z

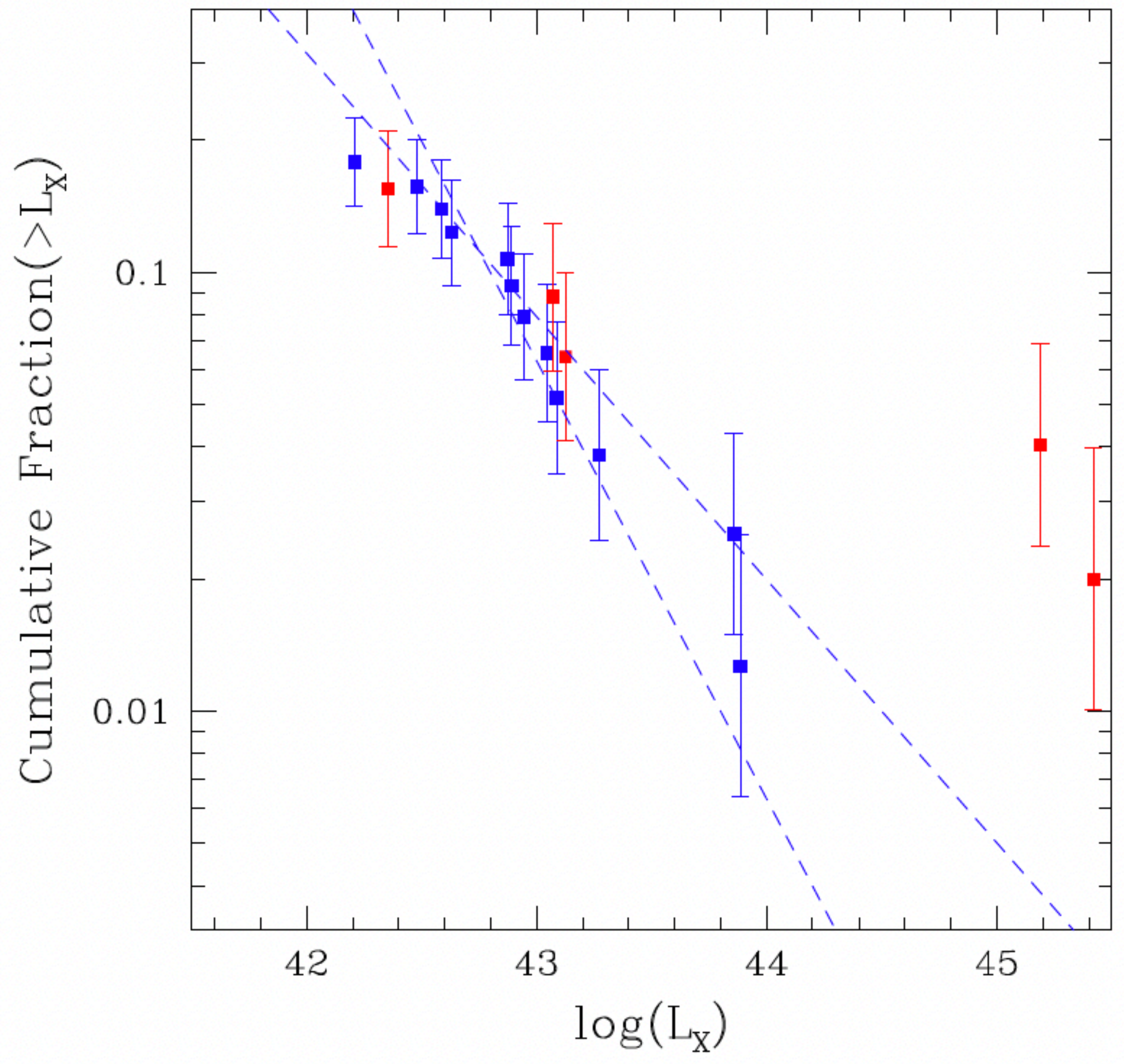

Figure 7. Cumulative fraction of X-ray luminous BCGs as a function of the hard-band L_X in the redshift range $0.2 < z < 0.3$ (blue squares) and $0.55 < z < 0.75$ (red squares). The two dashed lines bracketing the cumulative luminosity distribution in the low-redshift bin have slopes of -0.6 and -1.

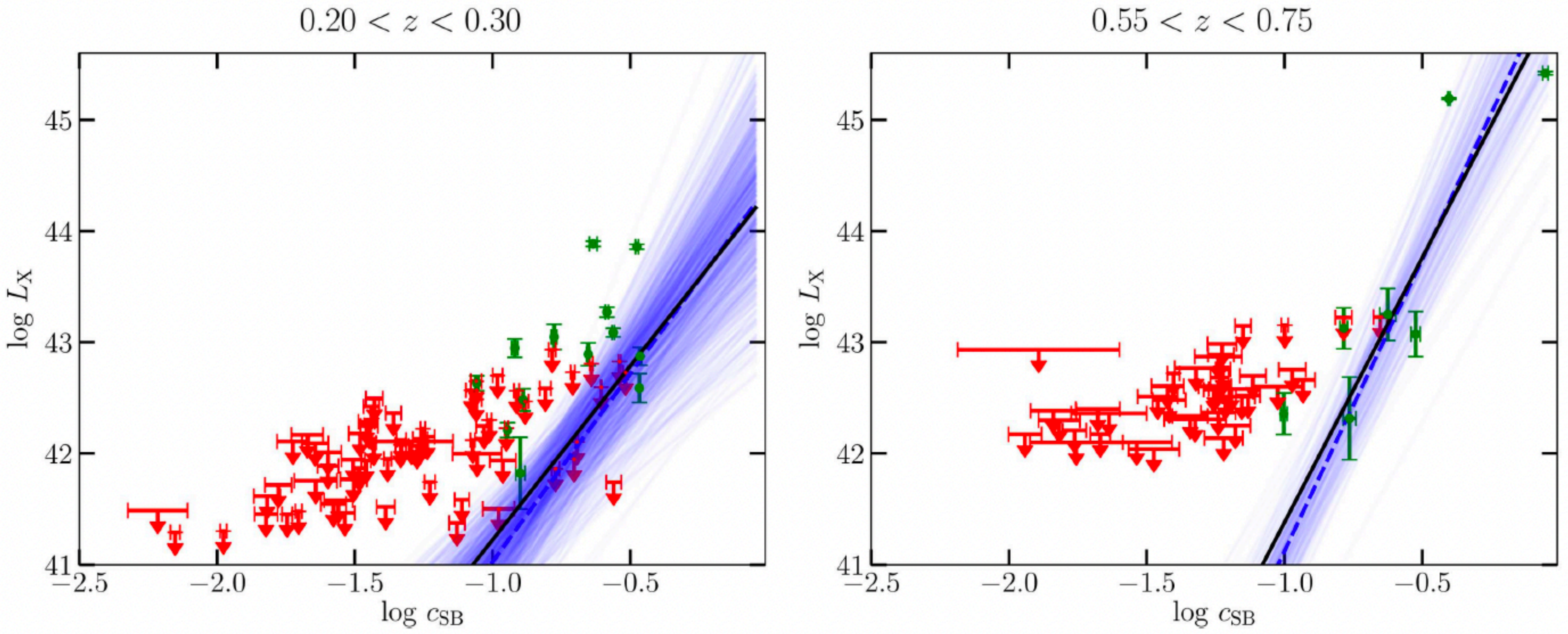

$0.20 < z < 0.30$
$0.55 < z < 0.75$
$\log L_X$
$\log c_{SB}$
45
44
43
42
41
−2.5
−2.0
−1.5
−1.0
−0.5

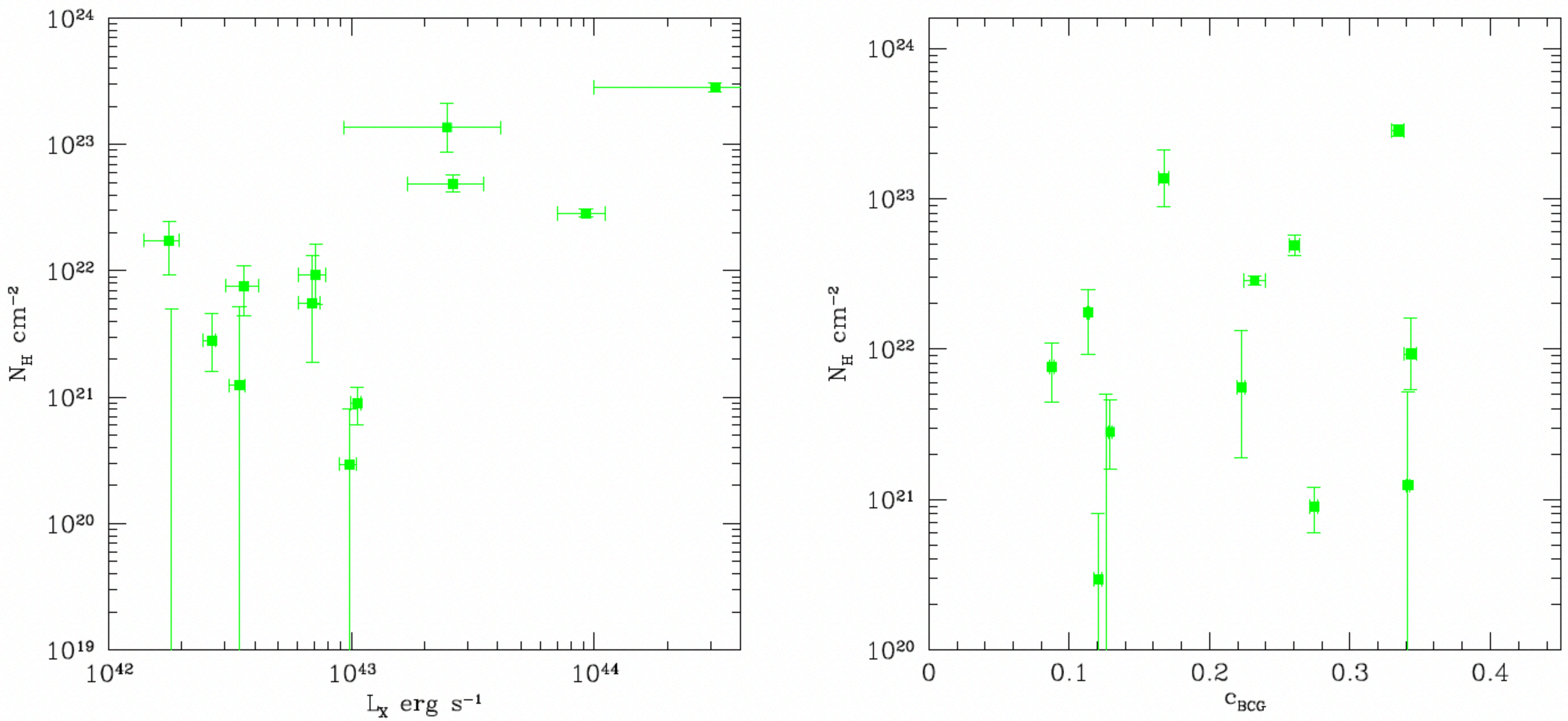

Figure 11. Left: intrinsic absorption N_H compared to the rest-frame 2–10 keV, unabsorbed luminosity as obtained from spectral analysis for the sources in the low-redshift sample. Right: intrinsic absorption obtained from spectral fits compared to the concentration parameter at the BCG position.

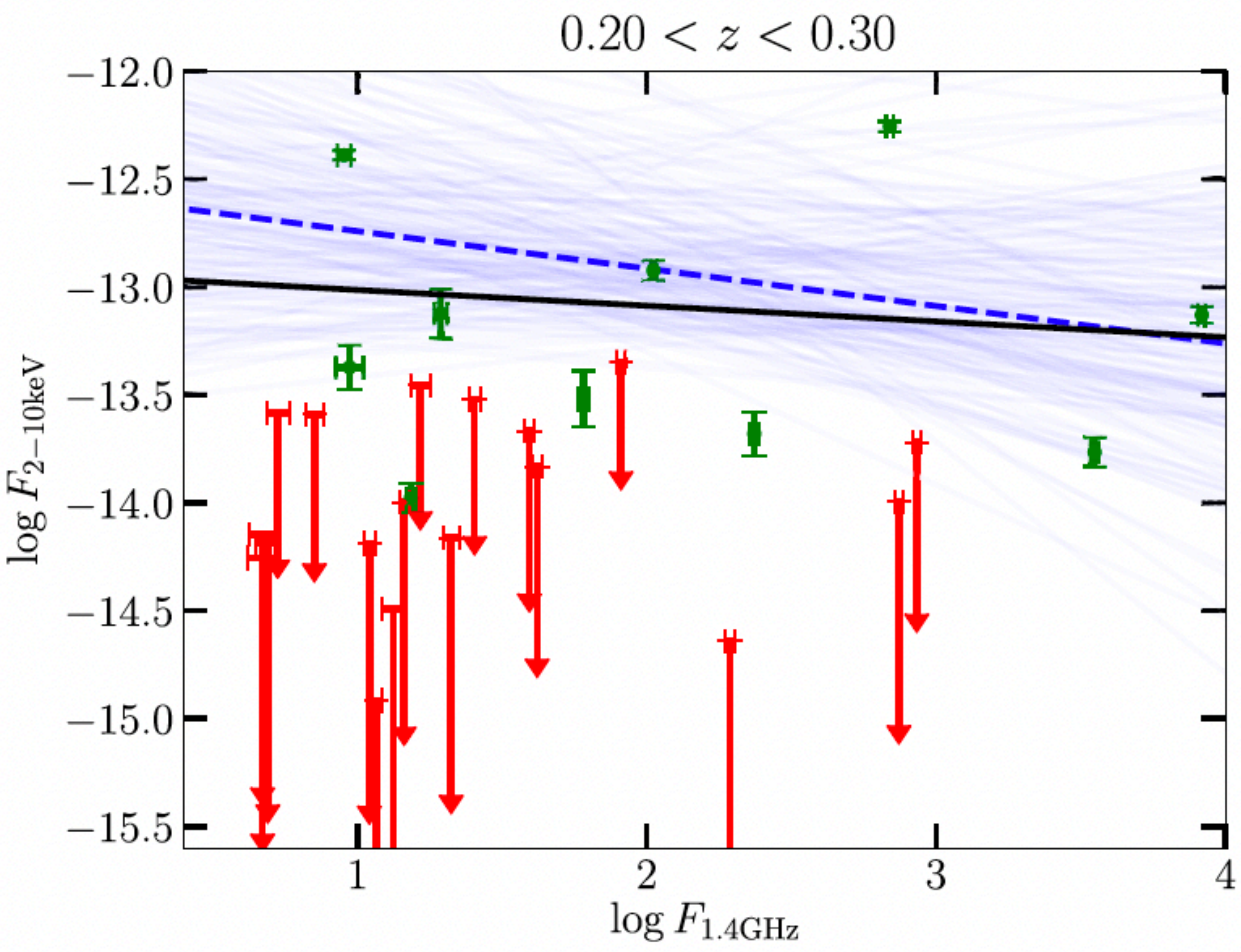

Figure 14. Results from the ASURV regression (solid black line) and the LINMIX_ERR (dashed blue line) on the correlation between hard X-ray flux and radio flux density at 1.4 GHz above 3 mJy. Light blue lines represent 200 different realizations of the relation from LINMIX_ERR.

Yu et al. 2018

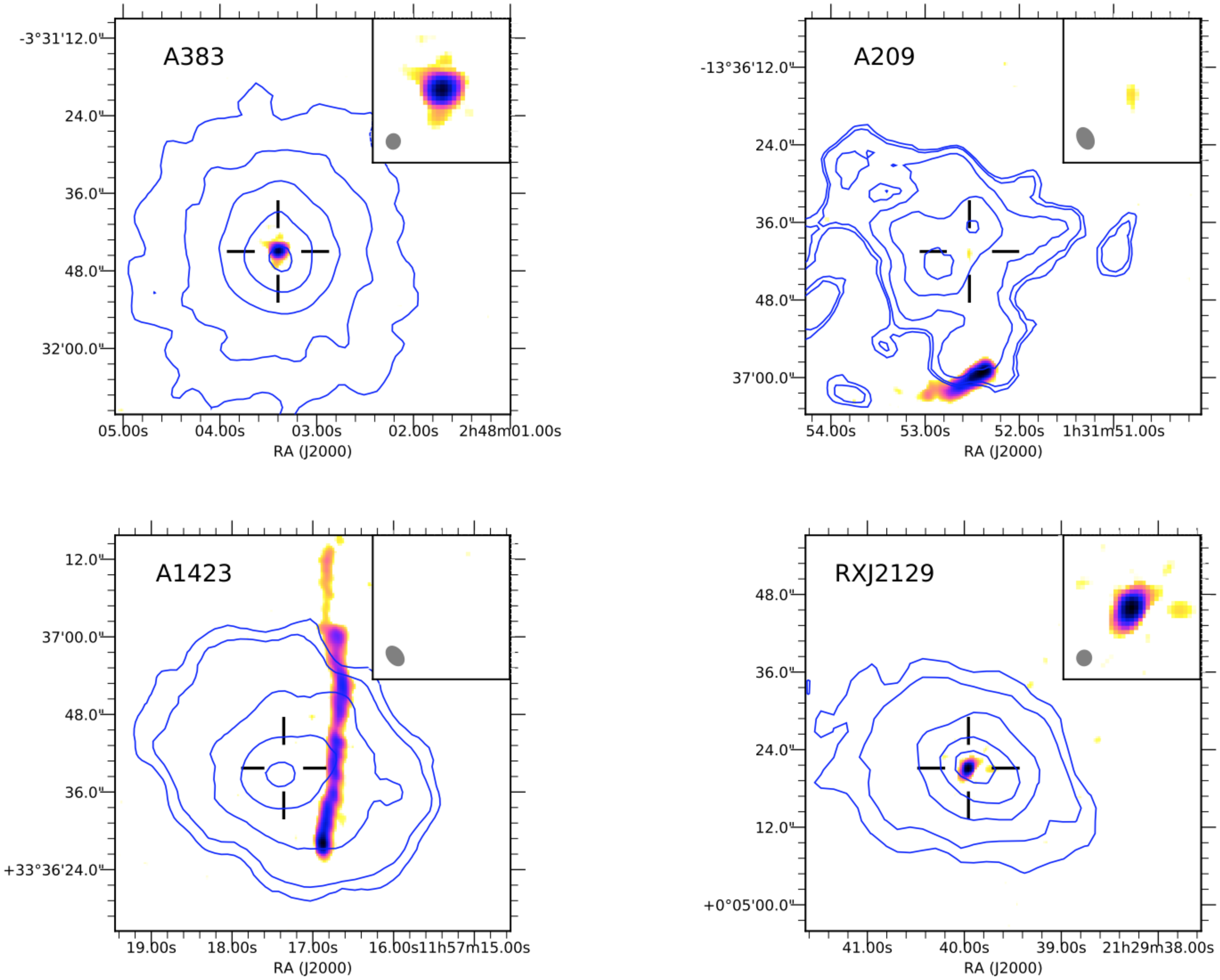
A383
-3°31'12.0"
24.0"
36.0"
48.0"
32'00.0"
05.00s
04.00s
03.00s
02.00s
2h48m01.00s
RA (J2000)
A209
-13°36'12.0"
24.0"
36.0"
48.0"
37'00.0"
54.00s
53.00s
52.00s
1h31m51.00s
RA (J2000)
A1423
12.0"
37'00.0"
48.0"
36.0"
+33°36'24.0"
19.00s
18.00s
17.00s
16.00s
11h57m15.00s
RA (J2000)
RXJ2129
48.0"
36.0"
24.0"
12.0"
+0°05'00.0"
41.00s
40.00s
39.00s
21h29m38.00s
RA (J2000)

Yu et al. 2018

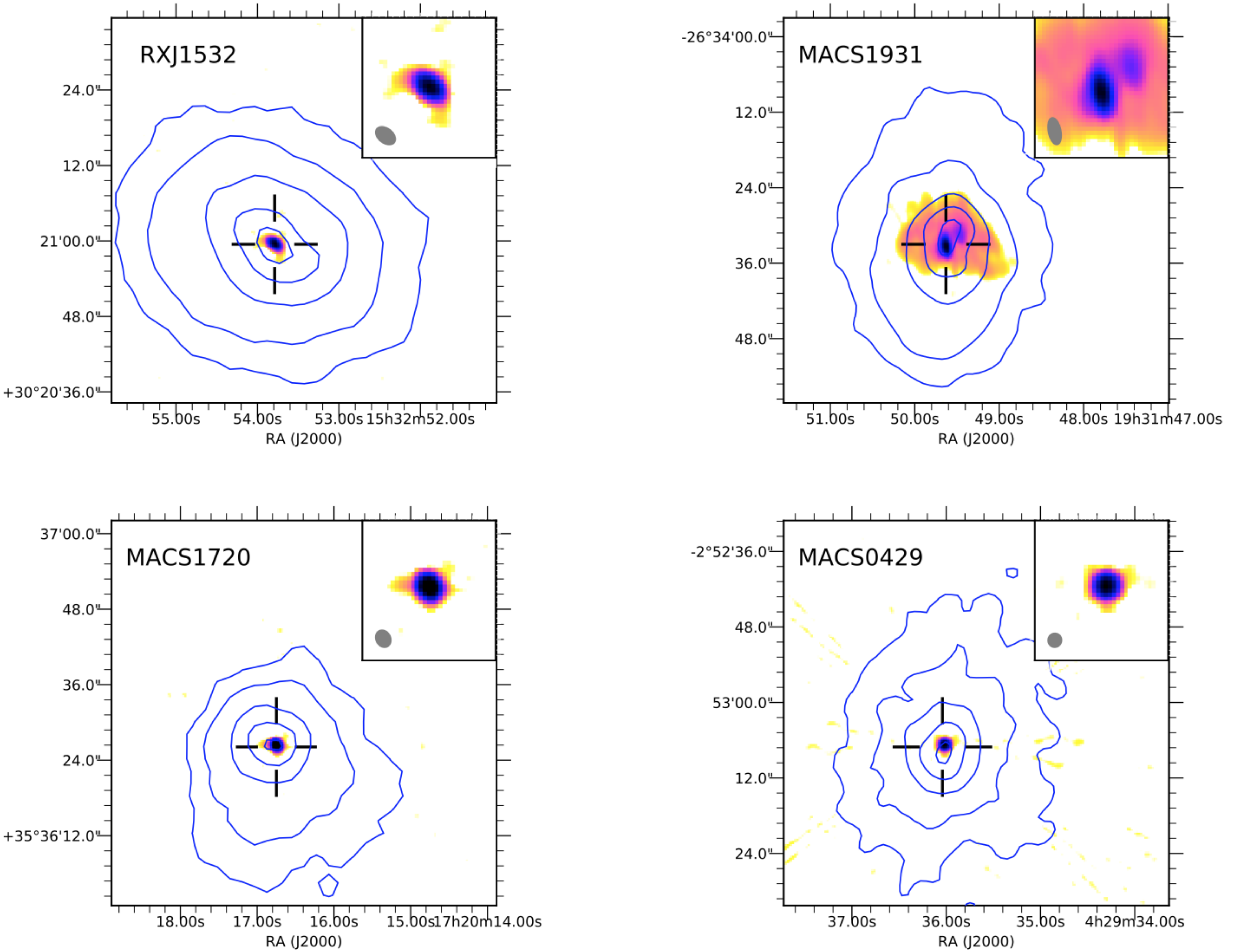
RXJ1532
24.0"
12.0"
21'00.0"
48.0"
+30°20'36.0"
55.00s
54.00s
53.00s
15h32m52.00s
RA (J2000)
MACS1931
-26°34'00.0"
12.0"
24.0"
36.0"
48.0"
51.00s
50.00s
49.00s
48.00s
19h31m47.00s
RA (J2000)
MACS1720
37'00.0"
48.0"
36.0"
24.0"
+35°36'12.0"
18.00s
17.00s
16.00s
15.00s
17h20m14.00s
RA (J2000)
MACS0429
-2°52'36.0"
48.0"
53'00.0"
12.0"
24.0"
37.00s
36.00s
35.00s
4h29m34.00s
RA (J2000)

Yu et al. 2018

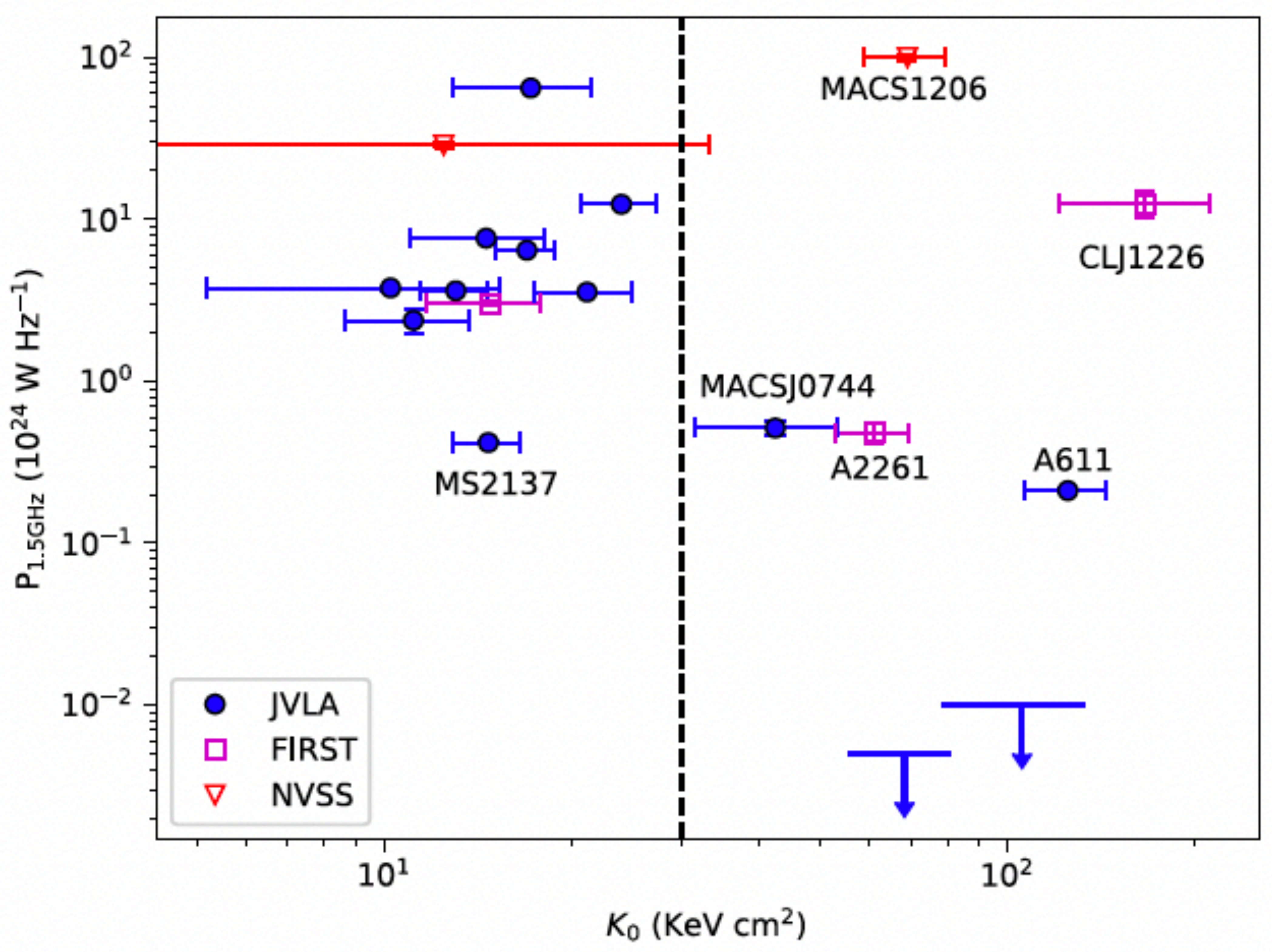

MACS1206
CLJ1226
MACSJ0744
A2261
A611
MS2137
JVLA
FIRST
NVSS
$P_{1.5GHz}$ (10^{24} W Hz^{-1})
K_0 (KeV cm^2)

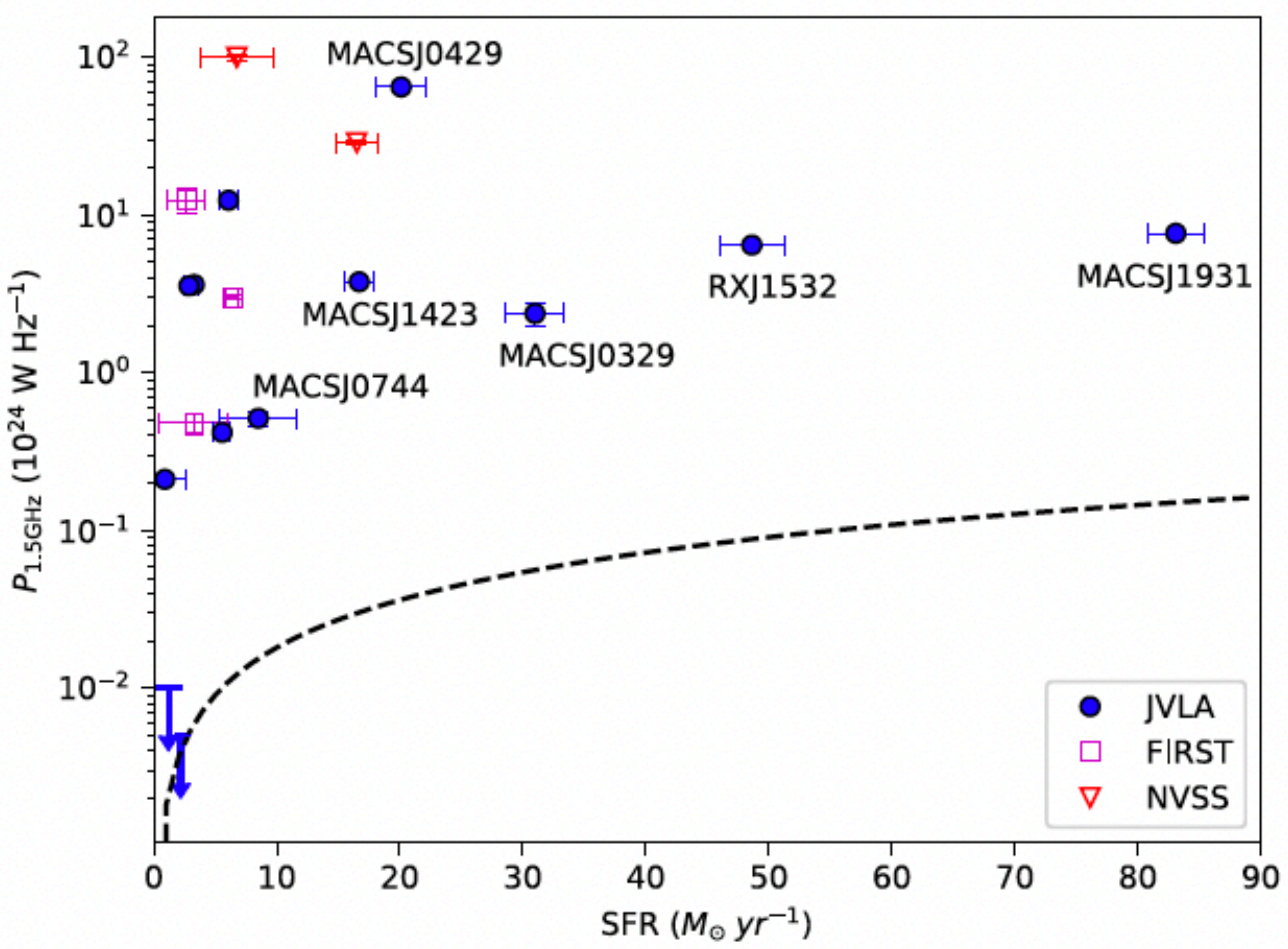

MACSJ0429
RXJ1532
MACSJ1931
MACSJ1423
MACSJ0329
MACSJ0744
JVLA
FIRST
NVSS
$P_{1.5GHz}$ (10^{24} W Hz^{-1})
SFR ($M_\odot$ yr^{-1})

BCGs). However, the finding that X-ray and radio luminosity correlate with BH mass in a significant manner only for those AGN in CC-BCGs suggests that their duty cycle – the time during which the AGN is active – is higher than that of AGN in NCC-BCGs and thus that they might be governed by a different accretion mechanism than that of NCC-BCGs.

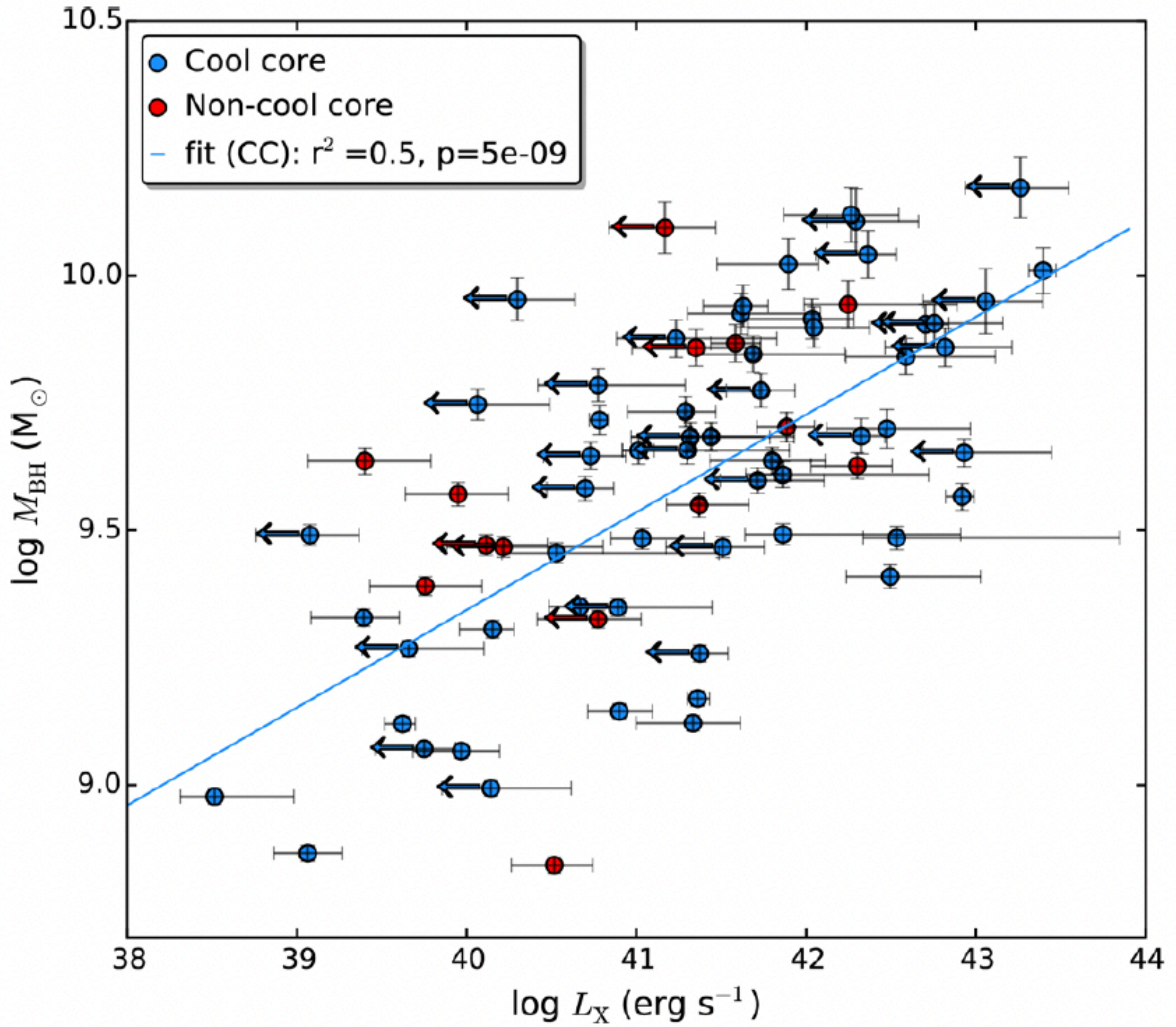

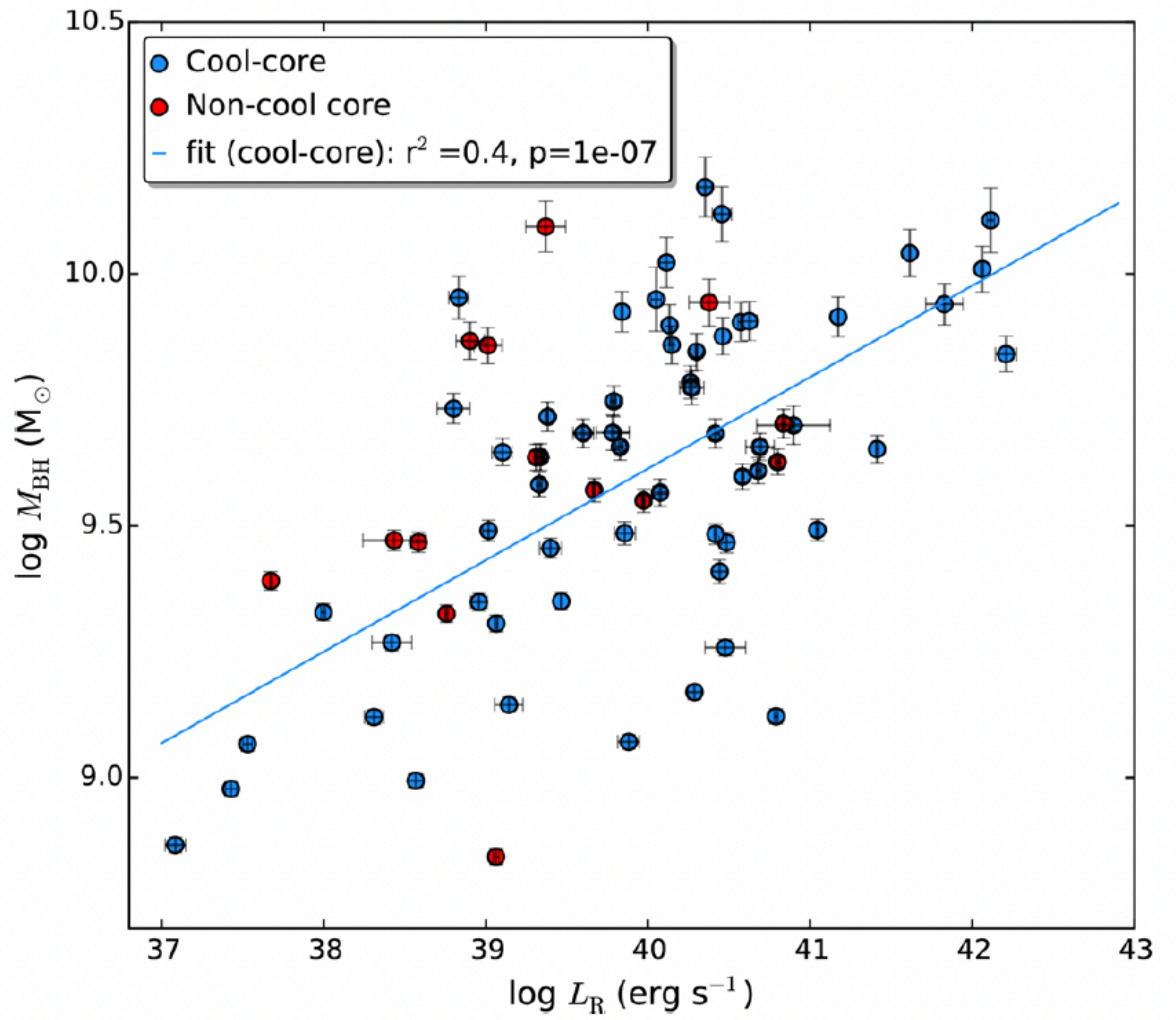

Mezcua et al. 2018

BCGs). However, the finding that X-ray and radio luminosity correlate with BH mass in a significant manner only for those AGN in CC-BCGs suggests that their duty cycle – the time during which the AGN is active – is higher than that of AGN in NCC-BCGs and thus that they might be governed by a different accretion mechanism than that of NCC-BCGs.

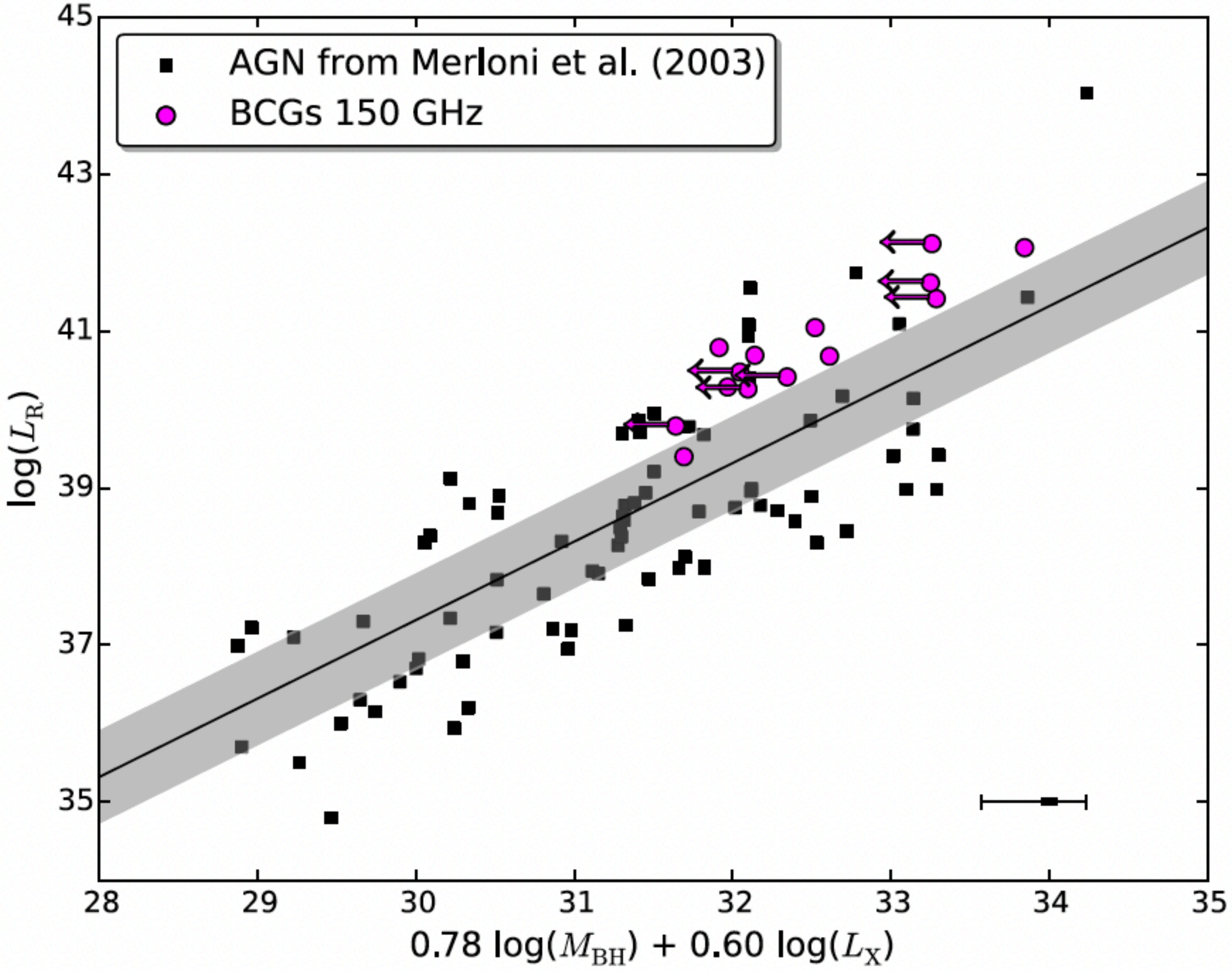

Mezcua et al. 2018

LX can heat and/or remove the gas in the very center of the BCG (radiative feedback) on a short time scale. But do we see radiative feedback in BCGs?

LR (through mechanical feedback) can heat the gas in the entire core region, reducing the reservoir of cold gas and quenching the cooling on a longer time scale.

LX and LR seem to correlate with MBH in CC clusters rather than in NCC, confirming cold accretion in addition to Bondi accretion, but also very much consistent with CCA, enhancing the duty cycle of AGN in CC clusters (but CC vs NCC classification is not accurate enough).

BCGs do not follow the fundamental plane of BH activity (LX, LR, MBH Merloni et al. 2003).

Can we describe the cycle with 2/3 parameters such as:

Feedback energy
- LX
- LR

Mass deposition rate

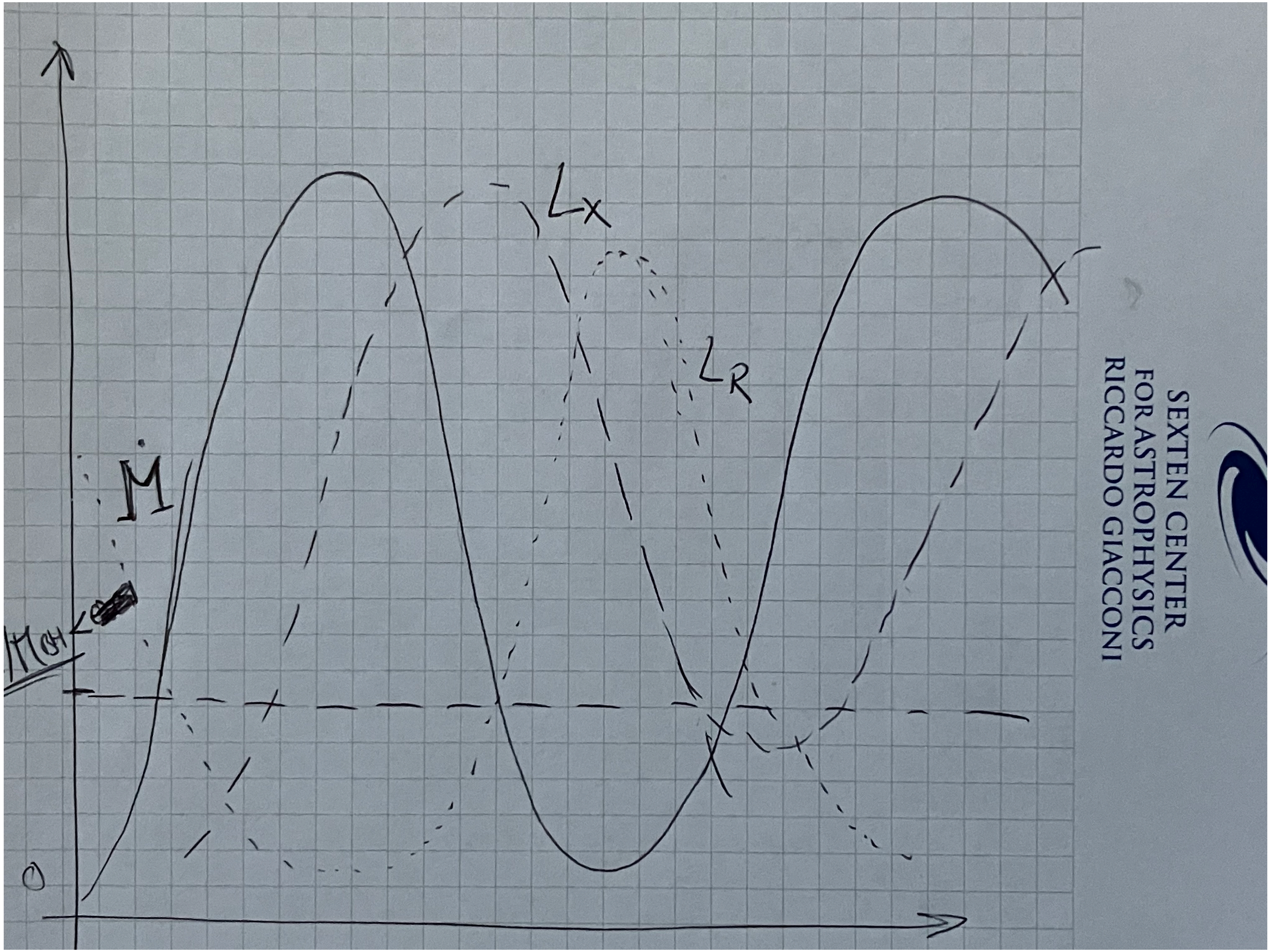

Dynamical complexity in astrophysical contexts - IFPU, Trieste 6-10 February 2023

The basic idea: the time delay between the onset of the mass flow, the accretion onto the SMBH, a radiatively-efficient phase, and the triggering of the radio-mode feedback
The phenomenology can be described with a Lotke-Volterra kind of equation?

$$\frac{dx}{dt} = Ax - Bxy$$

$$\frac{dy}{dt} = -Cy + Dxy$$

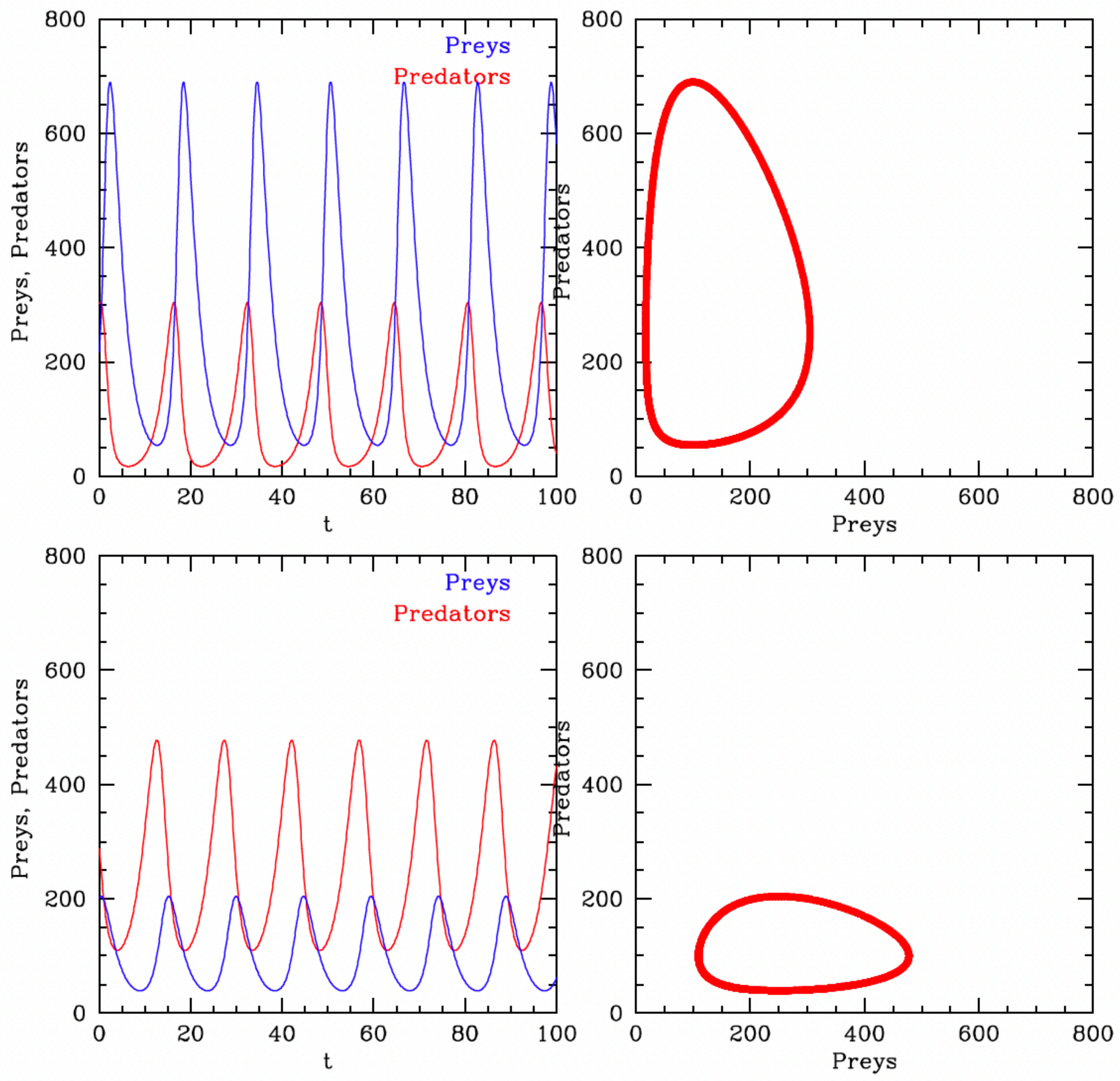

The plan:

Collect a sample (about 1000 of BCGs with M*, LR, LX, dotM (at different temperatures), MBH independently from M*?

Interpret the distribution of values in terms of orbits in a phase space ~ dotM vs LR/LX

An attractor for the ICM distribution

AN ATTRACTOR FOR THE DYNAMICAL STATE OF THE INTRACLUSTER MEDIUM

Diana Juncher[1], Steen H. Hansen[1], and Andrea V. Macciò[2]
[1] Dark Cosmology Centre, Niels Bohr Institute, University of Copenhagen, Juliane Maries Vej 30, 2100 Copenhagen, Denmark
[2] Max Planck Institut für Astronomie, Königstuhl 17, 69117 Heidelberg, Germany
Received 2011 November 15; accepted 2012 January 20; published 2012 February 6

$$M_{\rm tot}(r) = -r\frac{k_B T_g(r)}{\mu m_u G}(\gamma_g(r) + \tau_g(r)),$$

An attractor for the ICM distribution

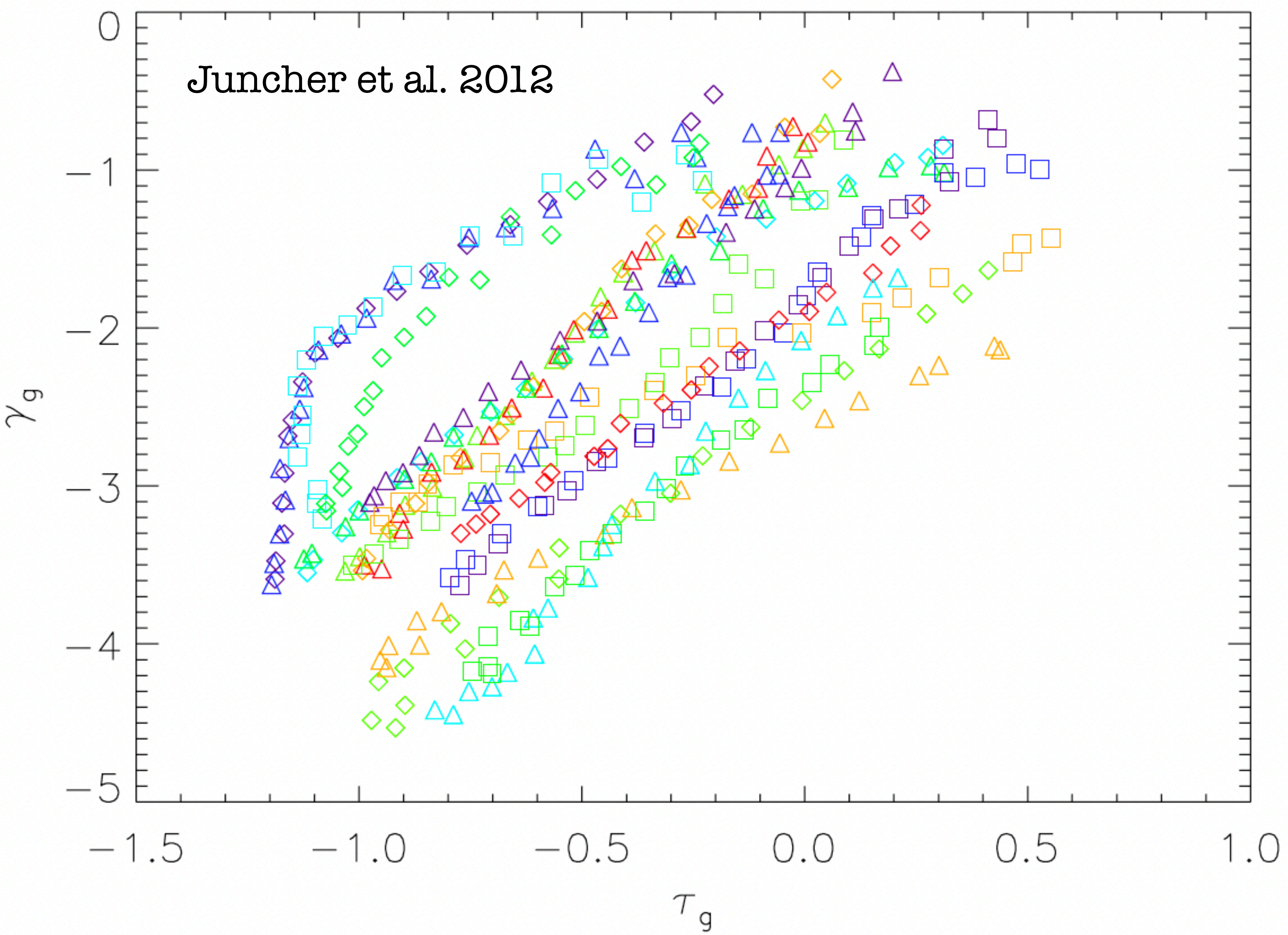

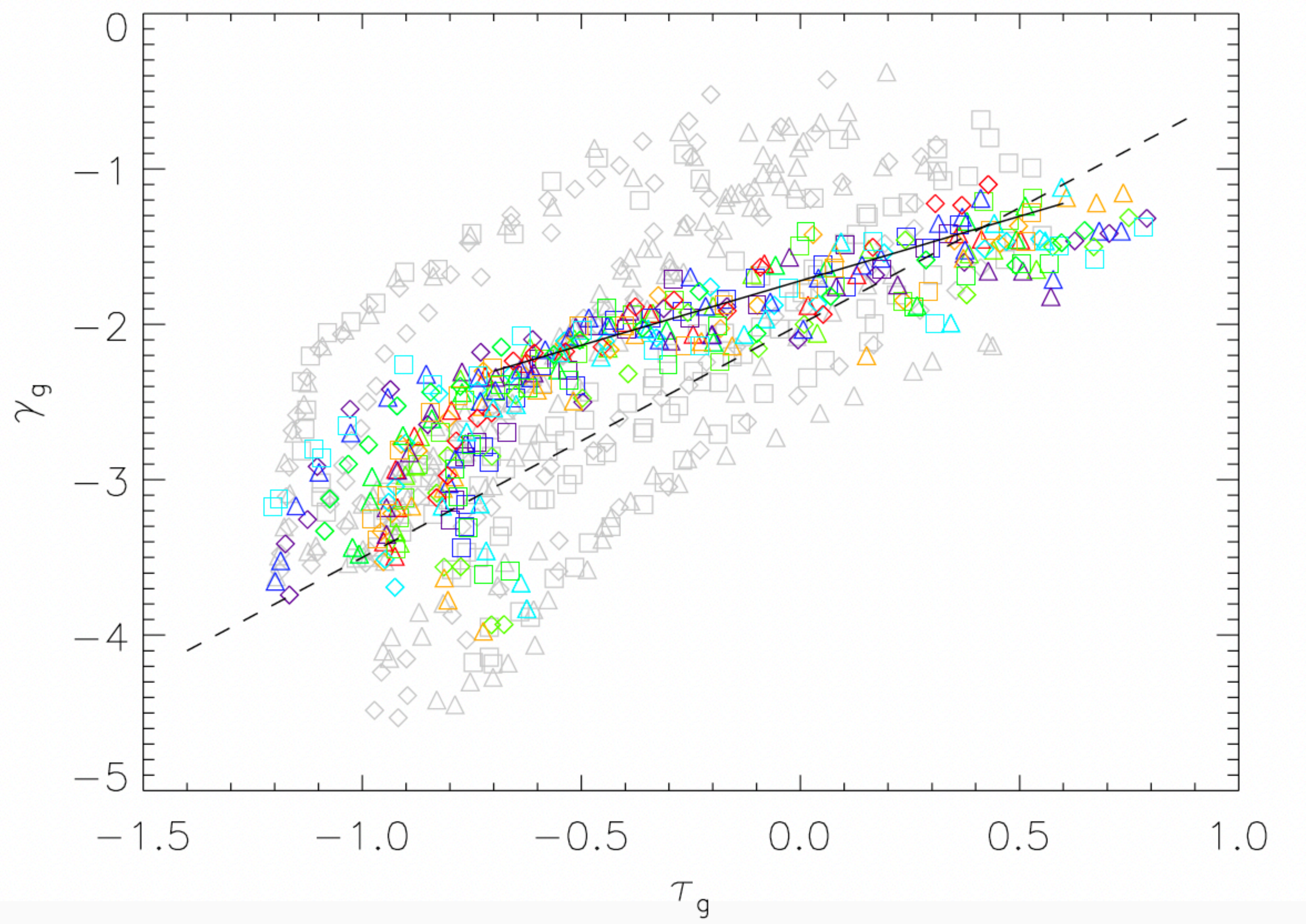

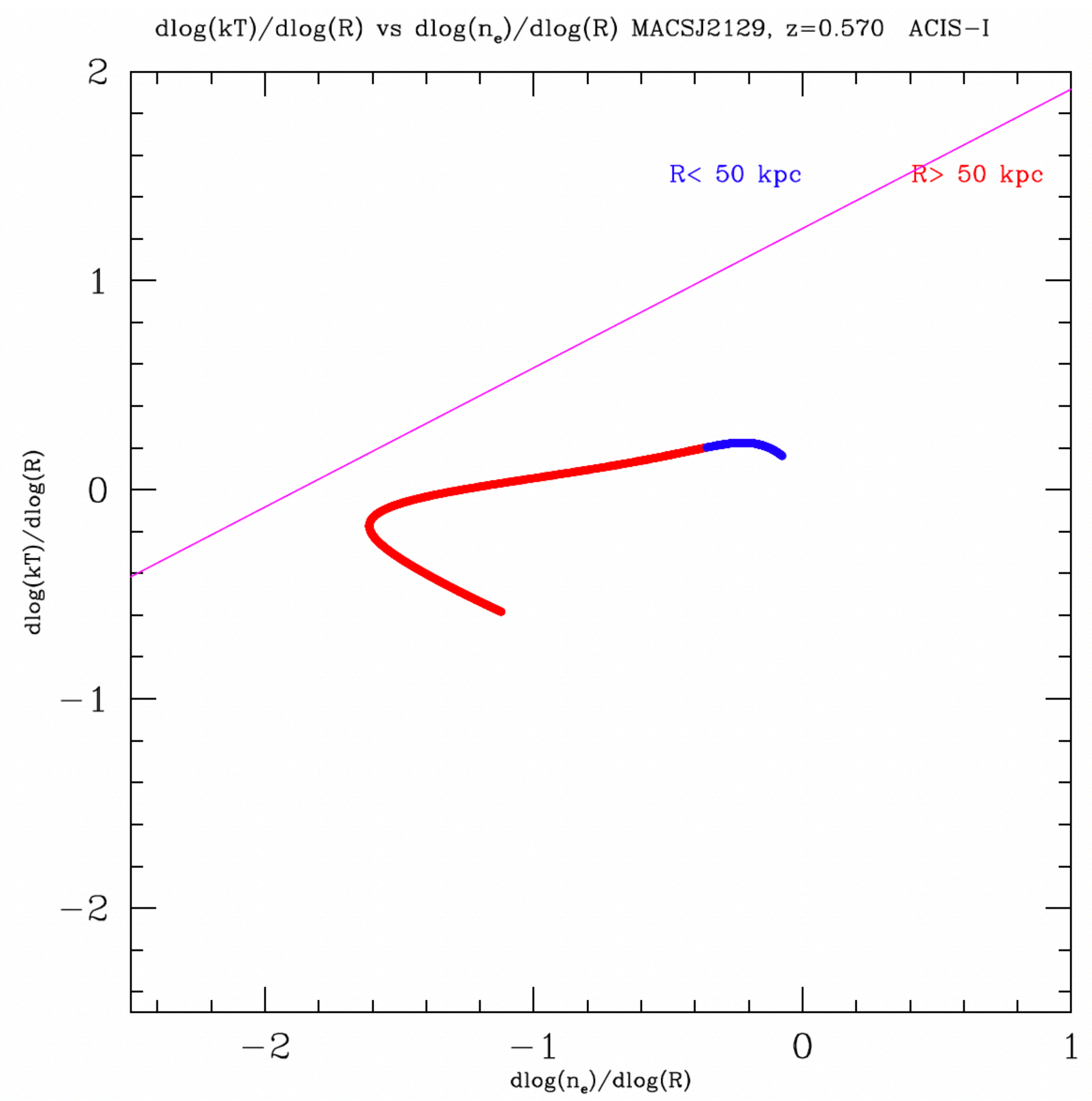
dlog(kT)/dlog(R) vs dlog(n_e)/dlog(R) MACSJ2129, z=0.570 ACIS-I
R< 50 kpc
R> 50 kpc
dlog(kT)/dlog(R)
dlog(n_e)/dlog(R)

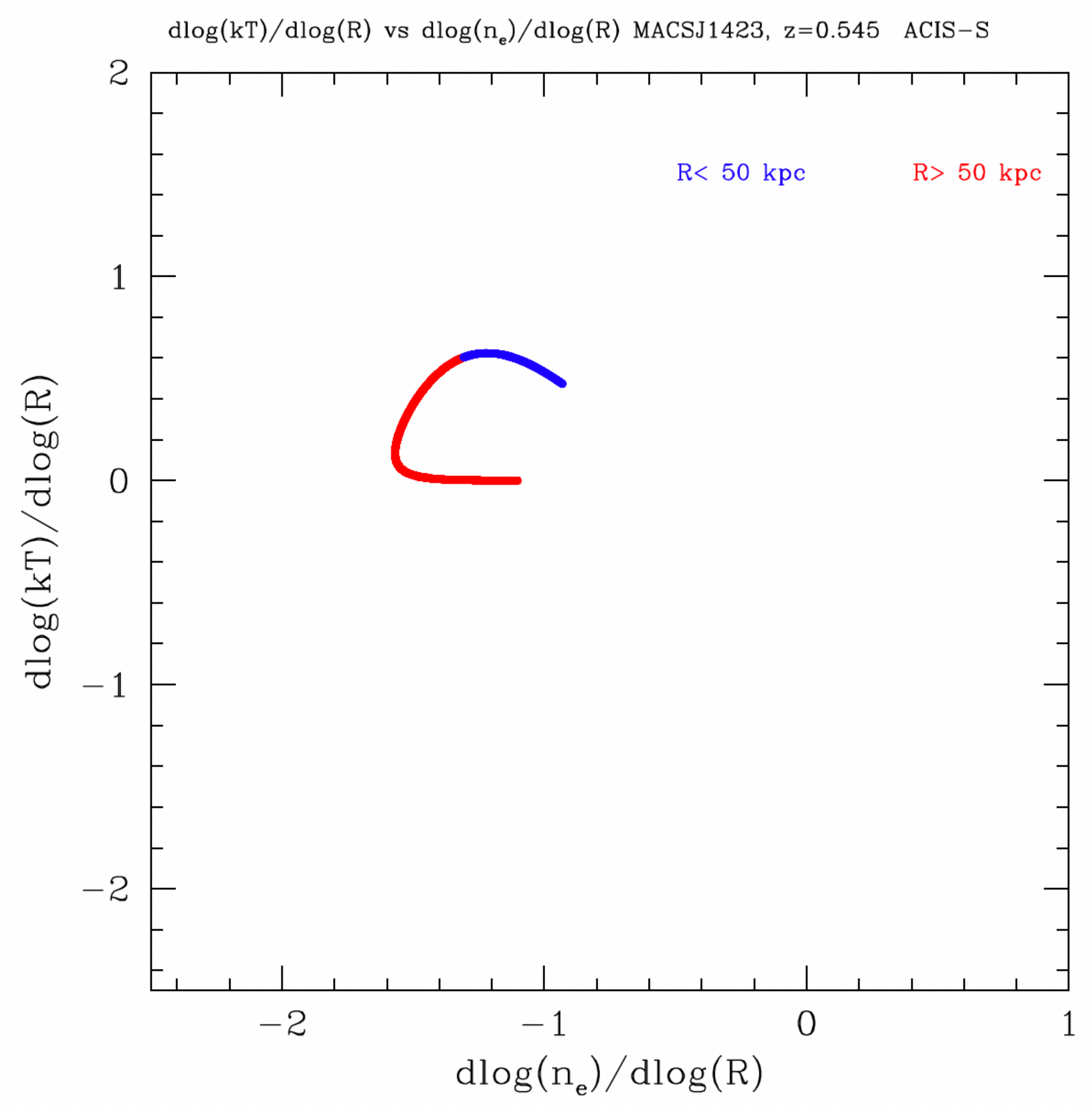
dlog(kT)/dlog(R) vs dlog(n_e)/dlog(R) MACSJ1423, z=0.545 ACIS-S
R< 50 kpc
R> 50 kpc
dlog(kT)/dlog(R)
dlog(n_e)/dlog(R)

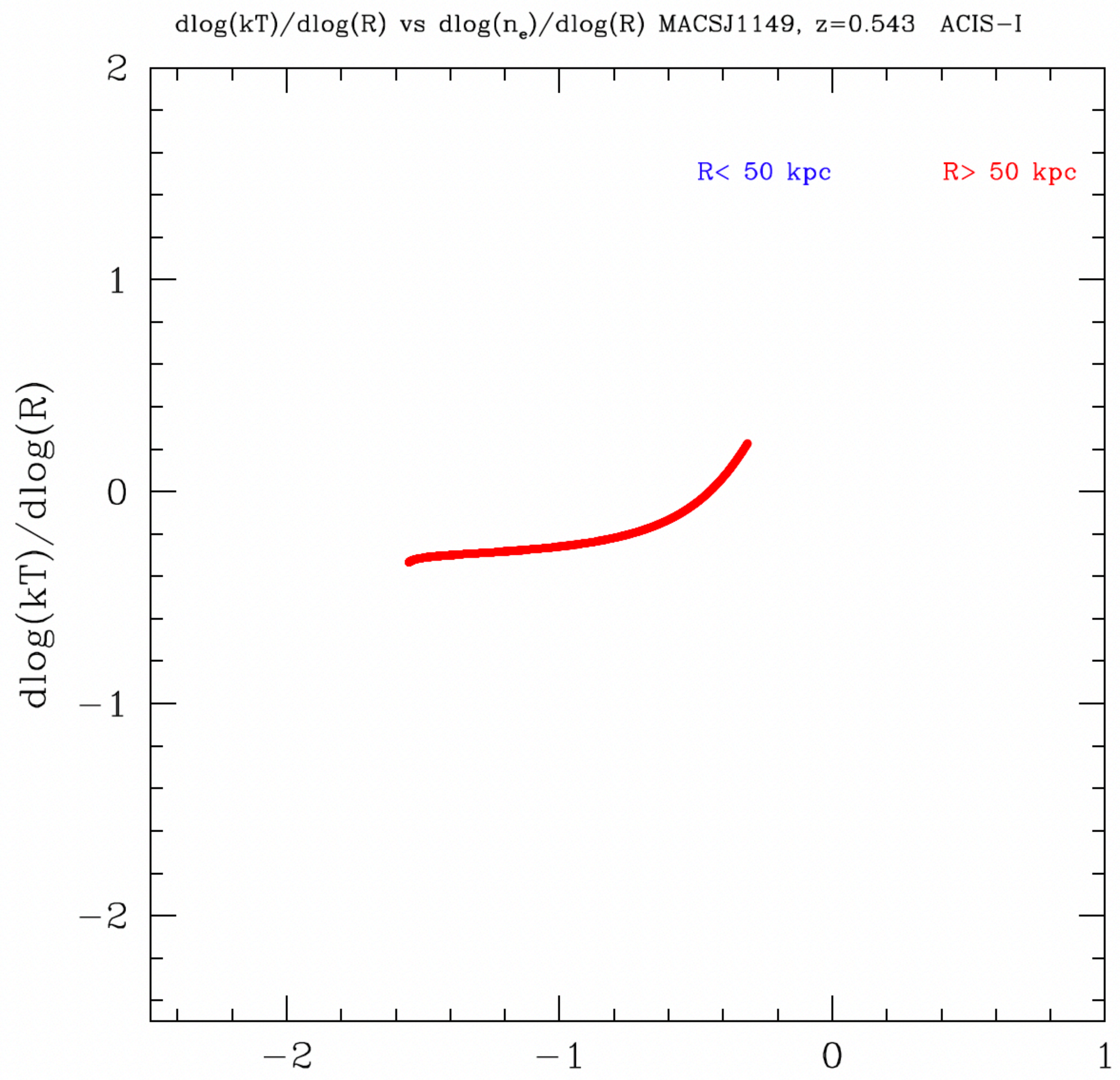
dlog(kT)/dlog(R) vs dlog(n_e)/dlog(R) MACSJ1149, z=0.543 ACIS-I
R< 50 kpc
R> 50 kpc
dlog(kT)/dlog(R)

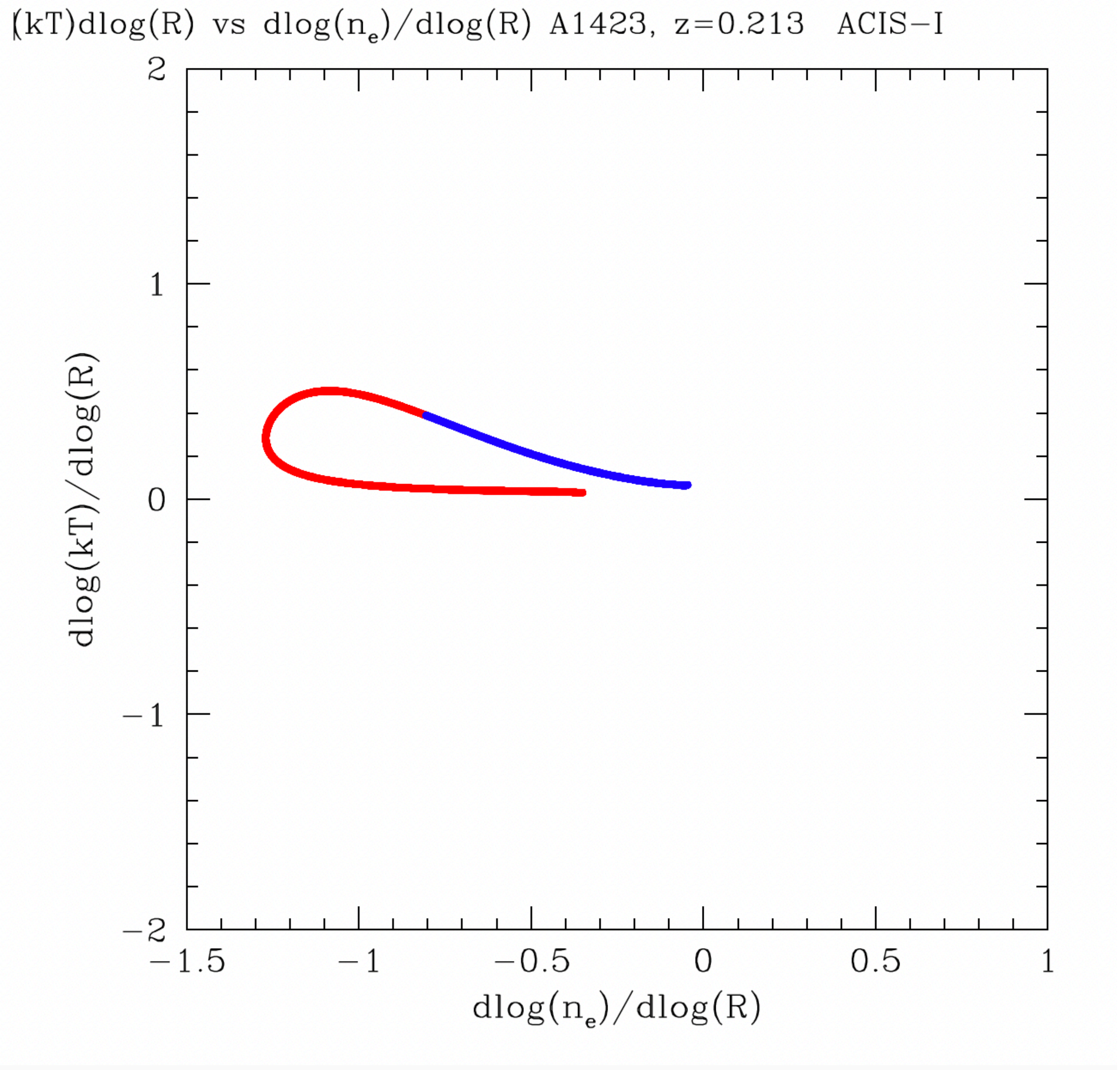
(kT)dlog(R) vs dlog(n_e)/dlog(R) A1423, z=0.213 ACIS-I
dlog(kT)/dlog(R)
dlog(n_e)/dlog(R)

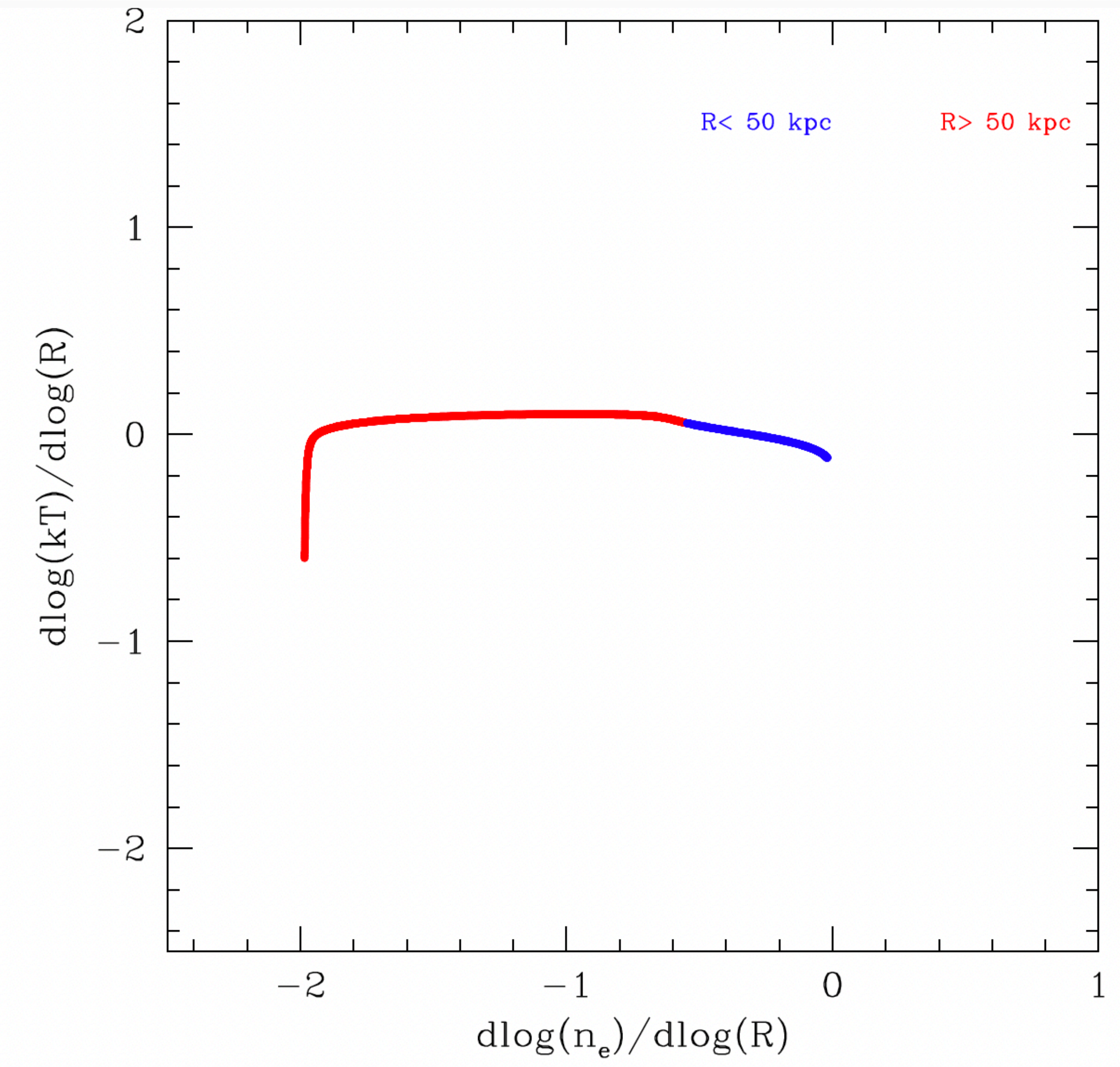
R< 50 kpc
R> 50 kpc
dlog(kT)/dlog(R)
dlog(n_e)/dlog(R)

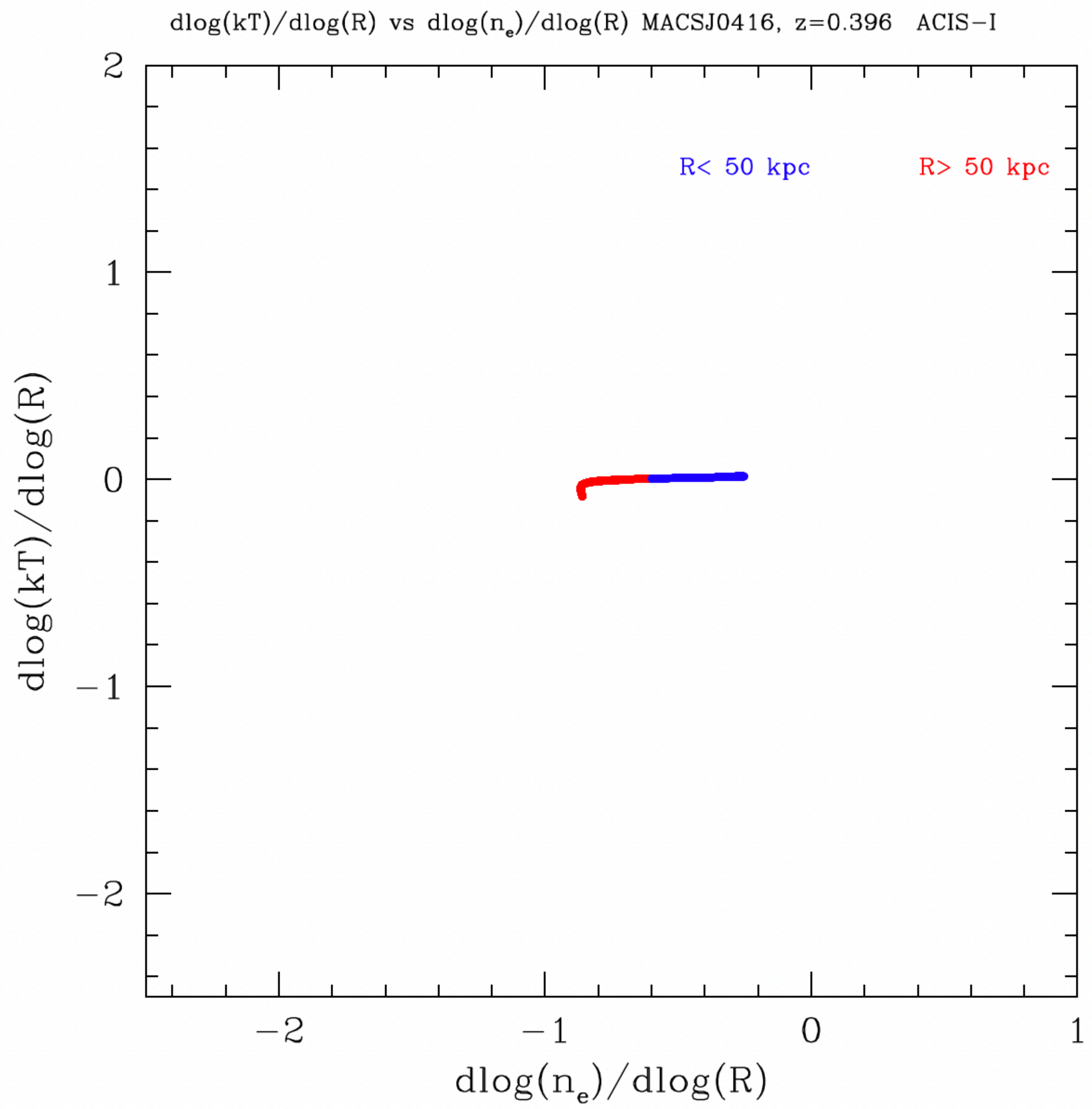
dlog(kT)/dlog(R) vs dlog(n_e)/dlog(R) MACSJ0416, z=0.396 ACIS-I
R< 50 kpc
R> 50 kpc
dlog(kT)/dlog(R)
dlog(n_e)/dlog(R)

Summary

Differently from massive, isolated galaxy, BCGs are heavily shaped by their environment during most of their secular evolution

The ICM-AGN system in BCGs - in regular clusters (without major dynamical disturbances) is an ideal system where we can observe emerging properties out of a very complex interlinked processes

The feeding process in the secular evolution of BCGs (after their formation at $1.5<z<3$) may be the key to understand the timescale of cooling/heating cycle

LX, LR and dotM (at different temperature/phases) can efficiently describe the system

An “attractor” in the ICM distribution linking temperature and density profile can provide an efficient mass proxy